Use of Remote Sensing in Assessment of Soil and Ecosystem Carbon Status

Yoshio Inoue
National Institute for Agro-Environmental Sciences, Tsukuba, 305-8604, Japan
e-mail: yinoue@affrc.go.jp

Abstract: Quantitative assessment of carbon exchange between terrestrial ecosystems and the atmosphere is one of the critical subjects in environmental policy-making as well as in related sciences since the carbon stock in ecosystems plays an important role in the global carbon cycle. Remote sensing is a vital tool for geospatial data acquisition for direct and indirect assessment of ecosystem carbon dynamics at local, regional and global scales. Remote sensing has unique merits compared the other methods i.e., especially in 1) wide area observation, 2) periodical and continuous measurement, 3) a wide range of spectral signatures are available, 4) digital data are suitable for processing, standardization, archiving and on-line distribution, 5) signatures from various sensors and platforms can be used synthetically, and 6) long-term and consistent archives allow chrono-sequential analysis. In this paper, the potential and practical use of remotely sensed signatures for assessment of soil and ecosystem carbon stock will be presented through some case studies.

Key words: ecosystem carbon stock, land-use, remote sensing, satellite, spectral signature

1. Introduction

Quantitative assessment of carbon exchange between various ecosystems and the atmosphere is one of the critical subjects in environmental policy-making (IPCC, 2003; Houghton et al., 2005; Hese et al., 2005; Ramankutty et al., 2007; Fung et al., 2007) as well as in related sciences since the carbon stock in terrestrial ecosystems plays an important role in the global carbon cycle (Tian et al., 2003; Dong et al., 2003; Bellamy et al., 2005). Organic carbon is closely related to crop productivity as well as to the physical characteristics of soils with regard to accelerated soil erosion processes (e.g., hydraulic conductivity and soil structure; Ben-Dor, 2008). Therefore, it is of interest to ecologists and land managers dealing with land degradation and environmental conservation issues (Ben-Dor, 2008).

Land-use changes such as conversion between cropland and forest may have great impacts on carbon exchange at the interface of land surfaces to the atmosphere (Houghton and Hackler, 1999; IPCC, 2003; Righelato and Spracklen, 2007; Meyfroidt and Lambin, 2008). Amazonian forest has been focused by many studies (e.g. Cochrane et al., 1999; Houghton et al., 2000; Hirsch et al., 2004; Davidson et al., 2008; Vargas et al., 2008). Nevertheless, estimating the carbon balance in many tropical regions remains an important challenge due to limited data and their uncertainty (Ramankutty et al., 2007). Various management practices in crop production such as tillage, cropping and irrigation, etc. have some additional effects on carbon balance in agro-ecosystems. The soil is one of the important carbon pools in the soil-vegetation/animal-atmospheric systems, and determined under interactive relations with water, biomass, residue and microorganisms, so that it may be reasonable to estimate the ecosystem carbon stock as a whole under each land-use, management and environmental condition. In other words, saptio-temporal assessment of ecosystem carbon status is essential for carbon sequestration strategies by terrestrial ecosystems as well as for sustainable crop production.

Remote sensing is a vital tool for geospatial data acquisition for direct and indirect assessment of ecosystem carbon dynamics at local, regional and global scales. Remote sensing has unique merits compared the other methods i.e., especially in 1) wide area observation, 2) periodical and continuous measurement, 3) a wide range of spectral signatures are available, 4) digital data are suitable for processing, standardization, archiving and on-line distribution, 5) signatures from various sensors and platforms can be used synthetically, and 6) long-term and consistent archives allow chrono-sequential analysis.

A great deal of efforts have been made to estimate biophysical variables such as biomass, net primary productivity (NPP) and light use efficiency as well as land-use change in a wide range of ecosystems (e.g. Dymond et al., 2001; Dong et al., 2003; Hese et al., 2005; Veroustraete et al., 2002). Spectral assessment of photosynthetic efficiency and capacity is one of vital interests in remote sensing and ecosystem science communities (e.g. Inoue et al., 2008a). Assimilation of remotely sensed data into biophysical process models would be another promising approach (e.g. Veroustraete et al., 2002; Inoue and Olioso, 2006; Dorigo et al., 2007). In spite of its usefulness, availability of optical satellite imagery is strongly limited due to the tropical climate conditions in the region, and the use of radar imagery (SAR) remains challenging due to the steep topographic conditions. The potential soil reflectance has been recognized by soil scientists, but the use of remote sensing for soil applications remains undeveloped and is seldom reported (Ben-Dor, 2008).

Thus, in this paper, the potential and practical use of remotely sensed signatures for assessment of soil and ecosystem carbon stock are presented through some case studies.

2. Spectral assessment of soil carbon content

The direct quantification of soil carbon content has been one of challenging applications of remote sensing. We attempted to explore the most useful spectral signatures for remote sensing of soil carbon content.

2.1 Materials and methods

2.1.1 Soils and spectral measurement

Reflectance spectra were obtained for a wide range of soil types in Japan. Ninety eight soil samples were taken from the specimens of soil monoliths collected by NIAES (Fig. 1). The carbon content for the soil samples ranged from 0.16 % to 19.8 % with overall average of 5.12 %. Soil reflectance spectra were obtained under laboratory conditions using a portable spectro-radiometer (FieldSpec-FR, ASD). Spectral range and the field of view of the sensor were 350-2500 nm and 25 º, respectively. Spectral resolution (full-width-half-maximum; FWHM) was 3 nm for the region of 350-1000 nm and 10 nm for 1000-2500 nm, while the sampling interval was 1.4 nm and 2 nm for each region, respectively. These signatures were used to derive spectra at 1 nm interval using cubic spline interpolation functions. We used these spectral data at 3 nm intervals in this study because they could carry the maximum information at narrow wavelengths. More than 10 measurements were made each

time, moving over the canopy, and averaged for spectral analyses. Spectral reflectance was derived as the ratio of reflected radiance to incident radiance estimated by a calibrated white reference (Spectralon, Labsphere).

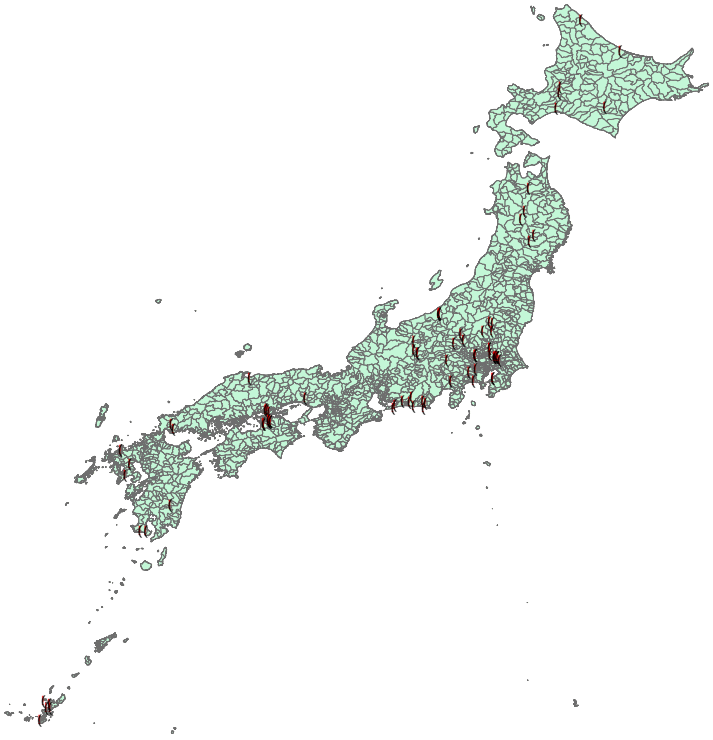

Fig. 1. Sampling sites of the soil monoliths specimens collected by NIAES.

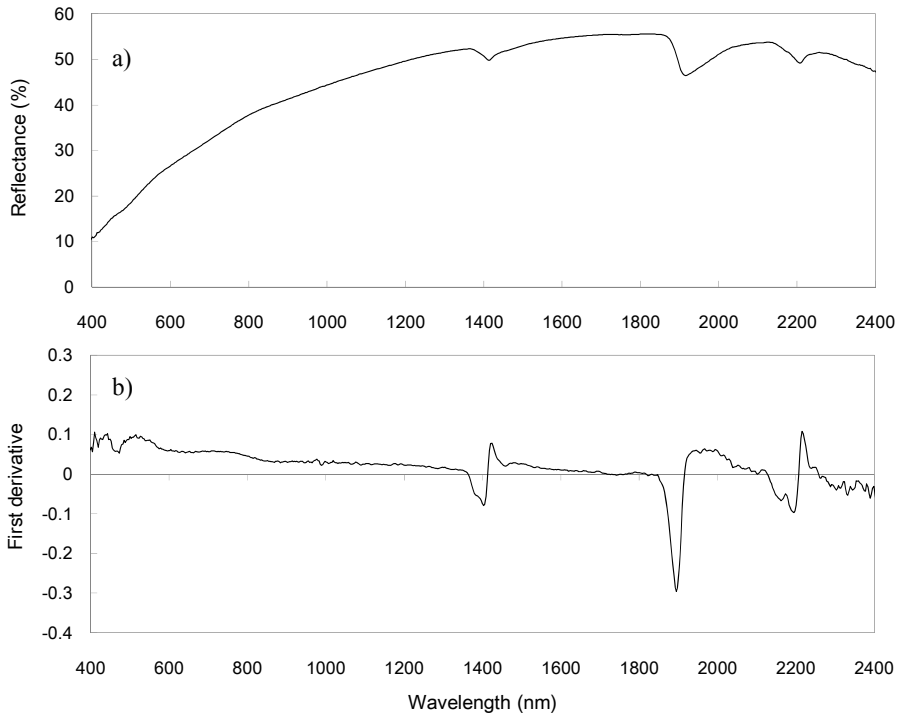

Fig. 2. An example of first derivative spectra of soil (b) derived from the reflectance spectra (a).

2.1.2 Analytical methods

Spectral indices using specific narrow bands

Normalization of reflectance values using a few wavebands is also effective to reduce the influence of errors or uncertainty due to sensor specification, atmospheric and background differences. First or second derivative spectra as well as reflectance spectra are used to extract local spectral features reducing the effect of trend or low frequency noises (Fig.2). The normalized difference spectral index (NDSI) is defined as;

$$NDSI\ (i, j) = (R_j - R_i) / (R_i + R_j) \qquad (1)$$

where, R_i and R_j are reflectance at i and j nm over the whole hyperspectra. Therefore, the most frequently used vegetation index NDVI is a specific case of NDSI using i = 660 nm and j = 830 nm. Similarly, the simple ratio index SRI (spectral ratio index) defined as;

$$SRI\ (i, j) = R_i / R_j \qquad (2)$$

is also often used in remote sensing; however, thorough combinations of the whole spectral bands is calculated in case of hyperspectra. These indices are simple but effective to reduce the influence of various errors. The NDSIs using reflectance values in vicinity have similar effects as first derivative. Both reflectance Ri nm and derivatives FDi nm can be used for these formulations.

Multivariate regression approaches

Multiple linear regression (MLR or ordinary least squares OLS) is often used to estimate a target variable from multiple variables. The structure of the model is as follows;

$$y_i = \beta_0 + \sum_{j=1}^{m} \beta_j x_{ij} + e_i \qquad (i = 1, \ldots, n; j=1, \ldots, m) \qquad (3)$$

y_i: target variable (dependent variable) x_{ij}: spectral reflectance (independent variables)
m: number of spectral bands n: number of samples e_i: error β_k: regression coefficients.

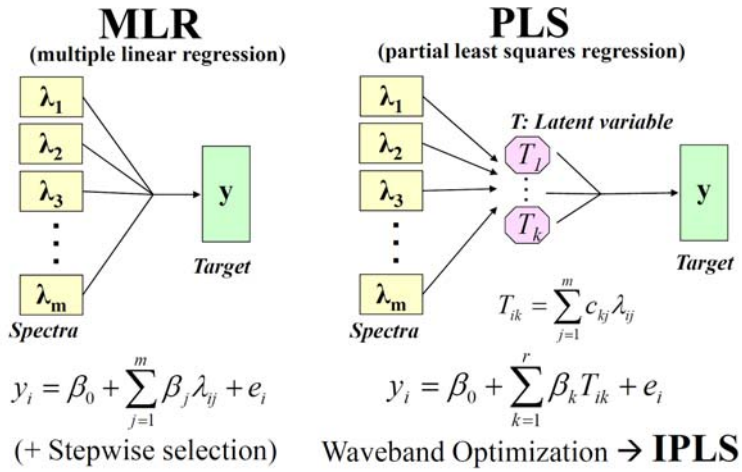

Fig. 3. Schematic diagram of multi-variable regression methods; MLR, PLS and IPLS.

The MLR assumes no inter-correlation between the independent variables, and in principle, the number of samples should be larger than the number of in dependent variables (Fig.3). Therefore, if independent variables have significant correlations each other, MLR model is not stable due to the multi-collinearity (redundancy). Consequently, MLR may provide a good fitting model in calibration, but its predictive ability is sometimes poor when applied to independent datasets. Thus, MLR may not be suitable for analysis of hyperspectra since many wavebands have strong correlation each other and number of wavebands is sometime larger than that of samples.

In order to avoid such constraints in MLR, principal component regression method (PCR) and partial least squares regression method (PLS) are often used in chemometry. The structure of the PLS is expressed as follows;

$$y_i = \beta_0 + \sum_{k=1}^{r} \beta_k T_{ik} + e_i \qquad (i = 1,\ldots,n) \tag{4}$$

$$T_{ik} = \sum_{j=1}^{m} c_{kj} x_{ij} \qquad (k = 1,\ldots, r) \tag{5}$$

y_i: target variable (dependent variable) x_{ij}: spectral reflectance (independent variables)
m: number of spectral bands n: number of samples e_i: error β_k: regression coefficients.
T_{ik}: latent variable (LV) r: number of latent variables c_{kj}: coefficient for LV.

The set of coefficients c_{kj} is determined so that the covariance between T_k and y is maximized. The number of latent variable is determined to minimize the prediction error through validation. Both PCR and PLS have close structures and are able to avoid the multi-collinearity, so that both methods can be applied to such dataset that have large number of independent variables and they correlate each other and the number of samples are not large enough as in the case of hyperspectra. However, principal

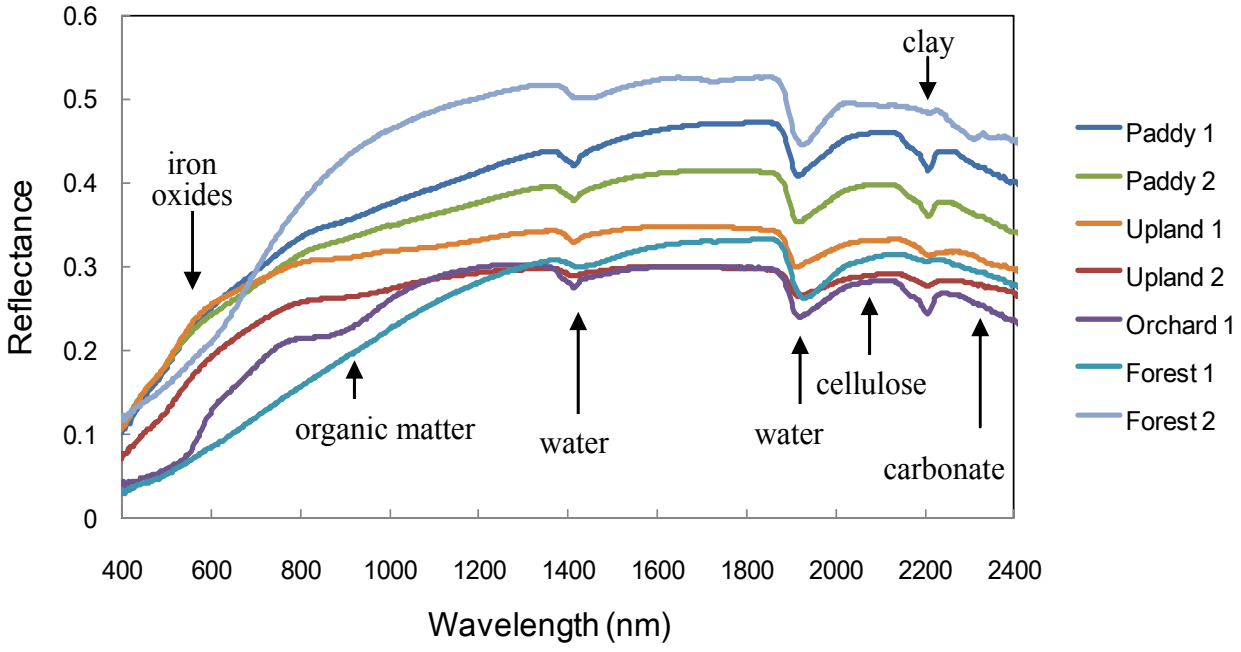

Fig. 4. Examples of soil reflectance spectra.

components in PCR are determined based on the variance of independent variables only whereas LVs are determined taking the covariance between the independent and target variables into consideration. Hence, PLS may be more suitable for hyperspectral analysis with higher predictive ability than PCR.

The PLS is often applied to the whole hyperspectra, but it is presumable that some of wavebands are not informative of the target variable or even disturbing. Therefore, the selection of spectral bands is very important in use of hyperspectra. Some improved PLS methods such as IPLS are associated with systematic selection of useful spectral bands by iterative procedures using predictive error. These approaches may be more useful than PLS (Norgaard et al., 2000).

2.2 Results and discussion

Figure 4 shows the typical examples of hyperspectral reflectance of soils from the monoliths specimens. In general, soil spectra is characterized by a monotonous increase in the visible region with or without a smear absorption feature of iron and a changing slope due to organic matter content. In the near-infrared (NIR) and shortwave infrared (SWIR) regions, there are two strong absorption features near 1430 nm and 1930 nm caused by the hygroscopic moisture content. Additional moderate or weak absorption features in the SWIR region due to clay minerals (2200 nm), carbonate (2330 nm), salt or primarily minerals, and organic compounds in the soil. Absorption at 2100 nm is also observed due to cellulose when some plant litter is included in the soil. This absorption feature can be used to quantify the coverage of soil by plant residues using a spectral reflectance at 2000, 2100 and 2200 nm (Nagler et al., 2003). Overall, soil reflectance spectra are mainly affected by the contents of minerals

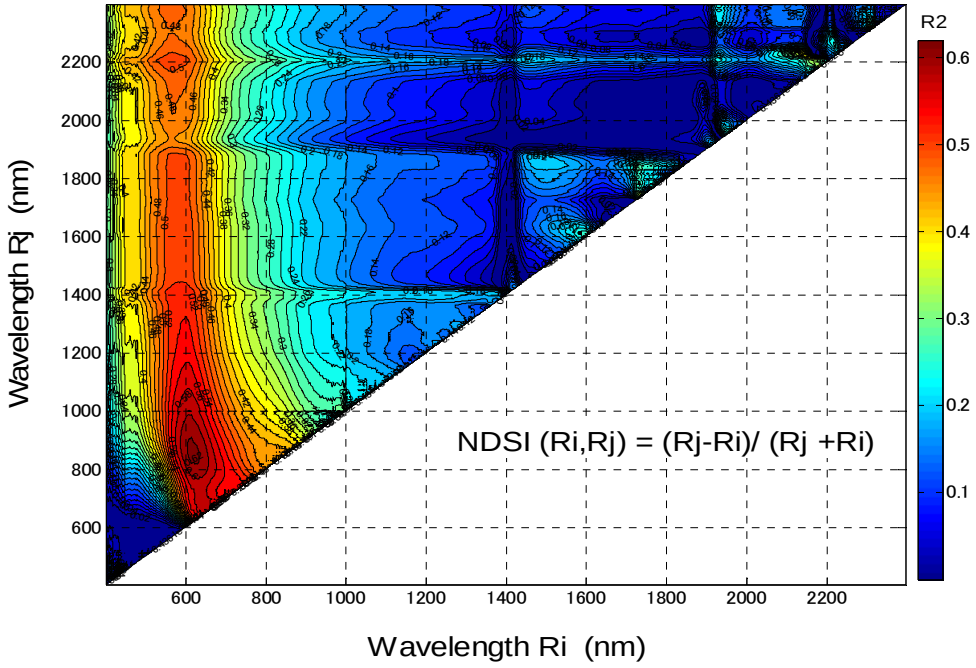

Fig. 5. Predictive ability of spectral indices NDSI (i, j) with thorough combinations of two wavelength Ri and Rj. This contour map indicates R^2 between NDSI (i, j) and soil carbon content.

(clay, iron oxide, primary minerals-feldspar, salt), organic matter (fresh and decomposing), and water (solid, liquid, and gas phases).

We explored most useful but simple spectral indices such as NDSI and SRI formulations using reflectance and FD values. Fig. 5 shows the NDSI map of predictive ability using reflectance values. The map provides useful insight on the position and width of the wavelengths regions that would be useful for assessment of soil carbon content. The spectral region (600 nm -620 nm) has relatively high predictive ability in wide range of combinations with wavelength over NIR-SWIR regions. Among the spectral combinations, we found that NDSI (868, 613) had the highest ability ($NDSI_{best}R$) in assessment of soil carbon content ($r^2 = 0.63$). The spectral width for the peak region is approximately 20 nm around 613 nm while 60 nm around 868 nm. These widths are not so narrow that some broad-band sensors may be used for prediction.

The best SRI also had similar level of predictive ability (r^2=0.62) at 841 nm vs. 622 nm at nearly the same position as $NDSI_{best}R$. Thus, the $SRI_{best}R$ was SRI (841, 622). It is obvious that the combinations of two bands within blue to green regions (400-550nm) and within the NIR-SWIR regions have poor predictive ability of soil carbon content.

Similar results were obtained using FD values in both NDSI and SRI formulations. The best NDSI using FD values ($NDSI_{best}FD$) was NDSI (FD763, FD445) with r^2 of 0.61. Therefore, taking FD may not be effective to improve the predictive ability compared to using raw reflectance values. On the other hand, the best SRI using FD values ($SRI_{best}FD$) showed the highest r^2 (=0.67) at 535 nm vs. 655 nm. Therefore, among these simple spectral indices, the SRI (FD535, FD655) had the highest predictive ability. Further investigation will be necessary, but the simple ratio index using first

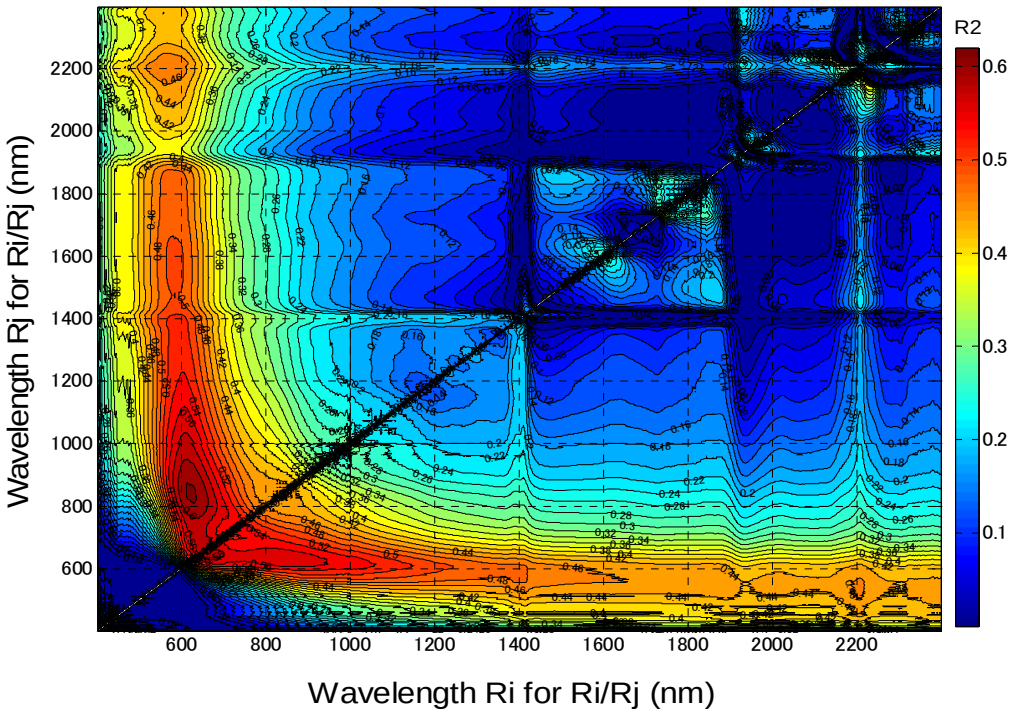

Fig. 6. Predictive ability of spectral indices SRI (i, j) with thorough combinations of two wavelength Ri and Rj. This contour map indicates R^2 between SRI (i, j) and soil carbon content.

derivative values at green and red spectral regions will be promising. Additional adjustment to these indices (e.g., SAVI to NDVI) may increase their predictive ability or robustness of these indices (Huete, 1988; Qi et al., 1994). The two dimensional maps of predictive ability NDSIs or SRIs using the thorough combinations of whole spectral bands are quite useful to understand the contribution of specific spectral bands and to explore the hot spots and their significant wavelength regions.

It was interesting that the PLS using the whole spectral wavelengths (667 bands) showed similar or less predictive ability (r^2 =0.53) as those simple indices using selected two bands. The PLS with iterative band selection (IPLS method) used only 15 wavebands, but had highest predictive ability (r^2 = 0.70; Fig. 7).

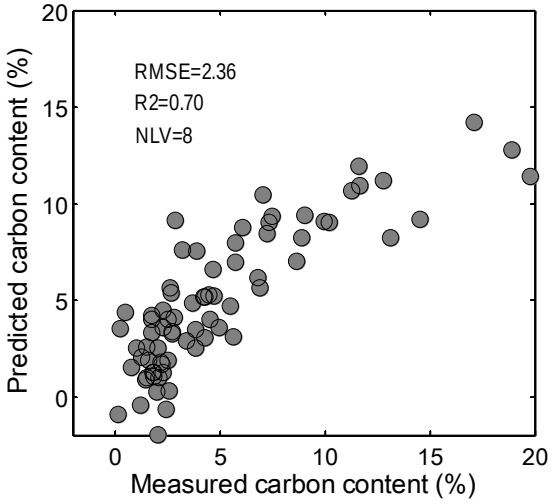

Fig. 7. Prediction of carbon content by an IPLS model using 15 wavebands.

2.3 Summary

We explored some powerful indices for prediction of soil carbon content using spectra signatures based on NDSI and SRI map approaches (Figs. 4 and 5). The best simple index was SRI using FD values 535 nm and 655 nm, i.e., SRI (FD535, FD655). The second best index was NDSI (868, 613). Both use the red wavelength region, so that it plays an important role in remote sensing of soil carbon. These normalization formulae using a few wavelengths would useful to reduce the atmospheric effects, sensor noise, and to enhance the sensitivity. It is interesting that the best NDSI or SRI have comparable or better predictive ability to those by PLS using the whole spectra or MLR using some selected bands. Another important result is that the IPLS with band selection had higher ability than PLS; that is, the use of whole spectra does not always provide the better result or even worse for prediction presumably because of some erroneous or disturbing spectral bands. The IPLS method may be the best approach in use of hyperspectra. Nevertheless, simple indices using selected wavebands by systematic selection method such as NDSI maps may also be useful especially when some limited number of wavebands are available. Results suggest the importance of waveband selection for each biophysical or geochemical target variables.

Simple experimental results clearly demonstrate that these methods are useful not only to find useful spectral indices or models but also to obtain insights on necessary wavebands and width or to design the spectral specification of future sensors. Whole spectra over a wide spectral range may not

be necessary to estimate individual target variables, but should be powerful to estimate various biophysical and biogeochemical variables at the same time since each target variable requires unique spectral index or model using different combinations of wavelengths.

3. Assessing land-use and ecosystem carbon stock using on time-series satellite images - a case study in slash-and-burn ecosystems in mountain of Laos -

In the tropical mountains of Southeast Asia, slash-and-burn (S/B) agriculture, i.e. shifting cultivation is an important food production system, and widely practiced in mountainous regions of Vietnam, Laos, China, Bangladesh, Myanmar, and northern India (Rasul and Gopal, 2003). In S/B agriculture, a patch of vegetation is cleared, burnt, and used to grow crops for a few seasons, and then abandoned for regeneration of vegetation. Hence, dynamic and large-scale changes in the ecosystem carbon stock occur over the cropping (C) + fallow (F) cycles. It has been pointed out that the S/B agriculture is a rational crop production system to utilize hilly lands with a little input, and used to be sustainable while the fallow period was long enough to recover the plant biomass and soil fertility (Fujisaka, 1991; Roder, 2001). The fallow biome also provides various non-timber forest products (NTFP; mushrooms, medicinal plants, bamboo, insects, etc.) that play an important role in rural livelihoods (Douangsavanh et al., 2006).

Nevertheless, increasing population pressure and land-use regulation have forced shifting cultivators to expand S/B areas and to shorten the fallow period (Pravongvienkham, 2004; Douangsavanh et al., 2006; Fujita and Phanvilay, 2008). Consequently, the negative effects on crop productivity such as decreasing soil fertility and increasing weed problems have been reported (Fujisaka, 1991; Roder, 2001), but also the negative impacts on biological resources (forest, NTFS, biodiversity, etc.) and the atmosphere are serious concerns. Therefore, alternative land-use and ecosystem management scenarios are urgently required to improve food and resource security (Douangsavanh et al., 2006) as well as for carbon sequestration. However, quantitative information on the chrono-sequential change of land use and ecosystem carbon stock in the region is not available. Limited accessibility to the mountainous areas as well as the limited availability of statistical data for the region has hampered scientific investigations, especially at regional scales (Fujisaka, 1991; Roder, 2001; Shrestha and Zinck, 2001). In general, it is difficult to obtain quantitative information especially on land-use history (Aumtong et al., 2009).

Thus, the main objective of this study was to provide quantitative information on the land use and ecosystem carbon stock in the region by linking time-series satellite imagery with an ecosystem carbon model derived from in situ experiments. Another objective was to infer the impacts of various land-use and ecosystem management scenarios on the potential of carbon sequestration at a regional scale. Due to the limitations in data availability as well as the difficult topographic conditions in the region, a simple approach using time-series satellite imagery examined by Inoue et al. (2007, 2008b) was applied for the geo-spatial assessment of land use and carbon stock in S/B ecosystems.

3.1 Study Area

The central part of northern Laos was selected as a study area (150×150 km; Fig. 8) not only because S/B agriculture is the major agricultural system there but also because the livelihood as well as natural

resources are dependent seriously on the S/B land-use in the area (Douangsavanh et al., 2006). Another reason is that the area is typical of similar ecosystems in the mountainous mainland region of Southeast Asia (Rasul and Gopal, 2003). The area is centred around 102°03'48.9" E, 20°13'12.8" N

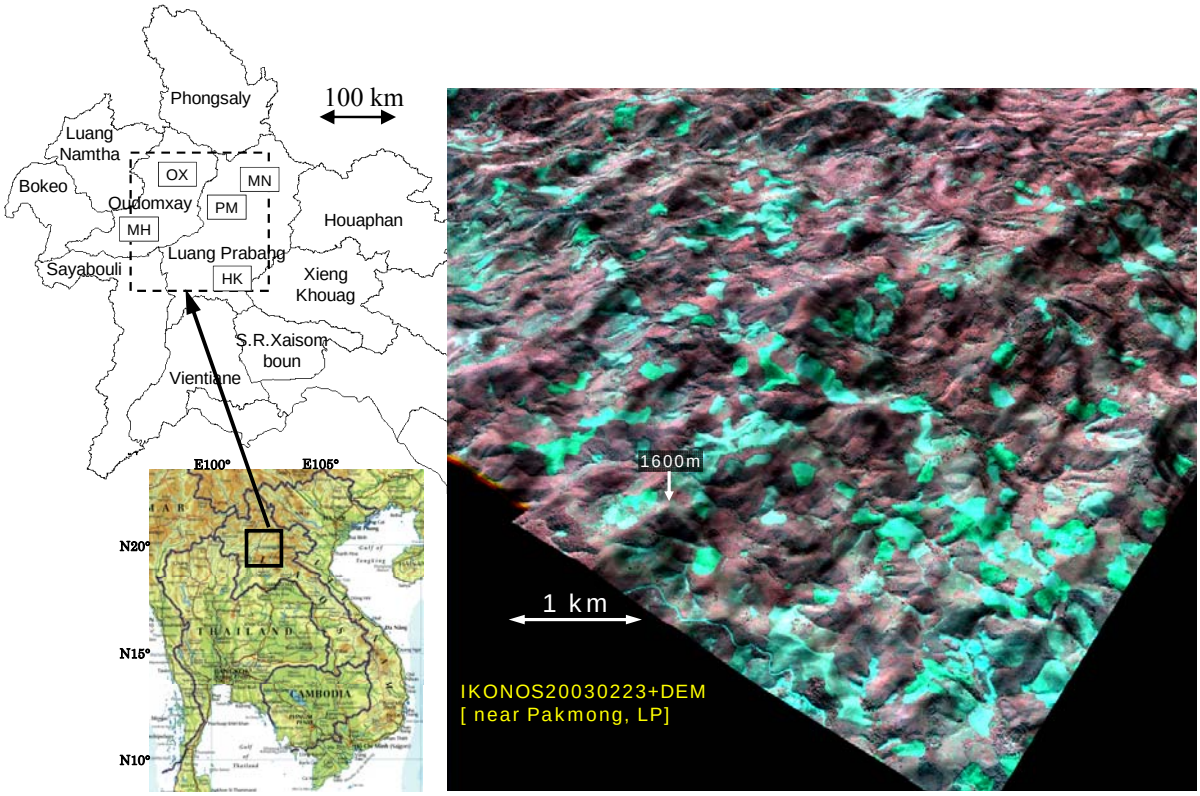

Fig. 8. The study area in northern part of Laos. A 3-D view generated from an image by a satellite IKONOS and digital elevation map shows one of the typical S/B areas in Luang Prabang province (February 23, 2003). The green, red, and near-infrared wavebands are assigned to B, G, and R colours, respectively. HK: Houaykhot, MN: Muang Ngoy, PK: Pakmong, OX: Oudomxay, MH: Muang Houn.

and is covered by a scene of Row46/Path129 of Landsat-TM. The elevation ranges from 300 to 2000 m, with a slope from 40 to 100 %. The mean annual rainfall for the area is about 1300 mm with the annual variability (SD) of 260 mm, but more than 90% of the rainfall is during the wet season from May to October. Soils of most S/B fields are classified as Orthic Acrisols, with a reddish-brown colour, clay contents > 30%, and a slightly acidic pH. Besides an extensive field surveys over the study area, an intensive study was conducted in a selected site in Luang Prabang Province (17.5×20 km; Houaykhot and Phonsavang villages).

Figure 8 shows the close bird's-eye view of a typical S/B region that was generated from digital elevation map and high-resolution satellite imagery. In this example, the emerald-green patches were used for slash-and-burn cropping during 2002, and reddish colour indicates the densely vegetated areas, respectively. These S/B patches shift year by year within the region, so that the potential area for S/B land use is much larger than the S/B cropping area in each year. In general, new land patches are

slashed during mid-February to early-March, burnt by mid-April, seeded during mid-April to May periods, and harvested during October to November periods. The most important crop in the area is upland rice, and some other crops such as Job's tear, sesame, and paper mulberry are also grown. Major tree species include *Irvingia malayana* and *Castanopsis echinocarpa* (Kiyono et al., 2007). Teak plantations were initiated in the area about 10-15 years ago.

3.2 Methodology

3.2.1 Reconnaissance

Ground-based information on land-surface conditions or land-use history was collected through field reconnaissance and interviews with villagers and officers during 2001-2006 periods. Major S/B areas in Luang Prabang, Oudomxay, and Luang Namtha provinces were visited during the dry seasons (October - April) in these years. Satellite images, digital maps, and geo-referenced photographs taken by cameras equipped with Global Positioning System were used to identify the land use at patch basis.

3.2.2 An approach to estimate S/B land use from satellite imagery

The region consists of some limited types of land use, i.e. S/B patches, fallow vegetation areas, conservation forests, spiritual forests (cemetery), roads, houses, paddy fields, teak plantations, and water bodies (river, pond). Conservation forests consist of the areas where S/B land use is basically prohibited by local government. Most dynamic spatio-temporal changes in land use occur among the S/B and fallow vegetation areas, while spatio-temporal changes as well as percentage area of the other types are minor. The S/B land use areas consist of a variety of cropping and fallow (C+F) patterns, and their area ratios are a crucial basis in this study. However, only qualitative information had been available from observation and interview (e.g. Roder, 2001; Douangsavanh et al., 2006), so that we derived such information from satellite imagery. Although it is not feasible to identify the age of fallow vegetation (community age = the number of years after abandonment) in a single satellite image, the S/B patches each year can be discriminated with high accuracy polygon-based classification (Inoue et al., 2007, 2008b). First, vector layers of polygons are generated from individual satellite images based on segmentation procedures using spectral signatures and morphological features. Next, the polygons are used for extracting S/B cropping patches based on supervised classification. The accuracy of this classification procedure proved as high as 0.95-1.0 (both producer's and user's accuracies) for the S/B land use (Inoue et al., 2007). This approach was applied to all satellite images consistently.

Landsat-MSS, TM and ETM+ satellite images (Row46/Path129) and high resolution images from IKONOS and QuickBird satellites over 33 years were used (Table 1). Due to the monsoon weather conditions, most images had been acquired during the dry season (November - April), and even a single image was not available in some of these years. High resolution images were acquired to cover several areas within the whole study region, and used for detailed analysis as well as for checking the classification results of Landsat images. S/B patches were extracted based on polygon-based classification of each Landsat image, and then used to produce a binary (S/B or non-S/B) image.

The classification results were checked using ground-survey information, observations, and high-resolution images. The binary images over consecutive years were stacked and used to trace the chrono-sequential change of S/B land use on a pixel basis. Consequently, the C+F land-use patterns (community age of fallow vegetation as well as timing and duration of S/B cropping) were derived at a pixel basis from the time-series analysis of satellite imagery only. In general, the polygon-based aggregation of pixels is reasonable and useful for this type of analysis (Wicks et al., 2002), but no previous studies adopted our approach presumably because high classification accuracy as well as the availability of time-series annual images for long period is required for this approach. Nevertheless, it was found feasible when applied to this type of ecosystems. In this dataset, the maximum traceable period was limited to the period between 1988 and 2005 since even a single image was unavailable in some years. Imagine 8.7 (ERDAS) and eCognition 5.0 (Definiens) were used for all image processing and analyses.

Table 1 Satellite images used for this study. Landsat images for 1988-2005 periods were used for the chrono-sequential analysis.

No.	Date (yyyy.mm.dd)	Sensor	No.	Date (yyyy.mm.dd)	Sensor	No.	Date (yyyy.mm.dd)	Sensor
1	1973.01.24	Landsat-MSS	13	1995.02.14	Landsat-TM	25	2002.02.28	IKONOS
2	1975.12.31	Landsat-MSS	14	1996.02.17	Landsat-TM	26	2002.11.08	Landsat-ETM+
3	1986.03.17	Landsat-MSS	15	1997.02.03	Landsat-TM	27	2003.02.23	IKONOS
4	1988.01.26	Landsat-TM	16	1997.11.02	Landsat-TM	28	2003.02.23	IKONOS
5	1989.03.25	Landsat-TM	17	1998.11.05	Landsat-TM	29	2003.04.03	QuickBird
6	1989.12.14	Landsat-TM	18	1999.01.24	Landsat-TM	30	2003.10.18	QuickBird
7	1990.01.31	Landsat-TM	19	1999.11.16	Landsat-ETM+	31	2003.12.05	Landsat-TM
8	1990.11.15	Landsat-TM	20	2000.03.07	Landsat-ETM+	32	2004.04.11	Landsat-TM
9	1991.04.08	Landsat-TM	21	2000.11.02	Landsat-ETM+	33	2004.12.07	Landsat-TM
10	1992.02.06	Landsat-TM	22	2001.02.06	Landsat-ETM+	34	2005.02.28	QuickBird
11	1993.02.08	Landsat-TM	23	2001.11.21	Landsat-ETM+	35	2005.11.24	Landsat-TM
12	1994.01.10	Landsat-TM	24	2002.02.09	Landsat-ETM+			

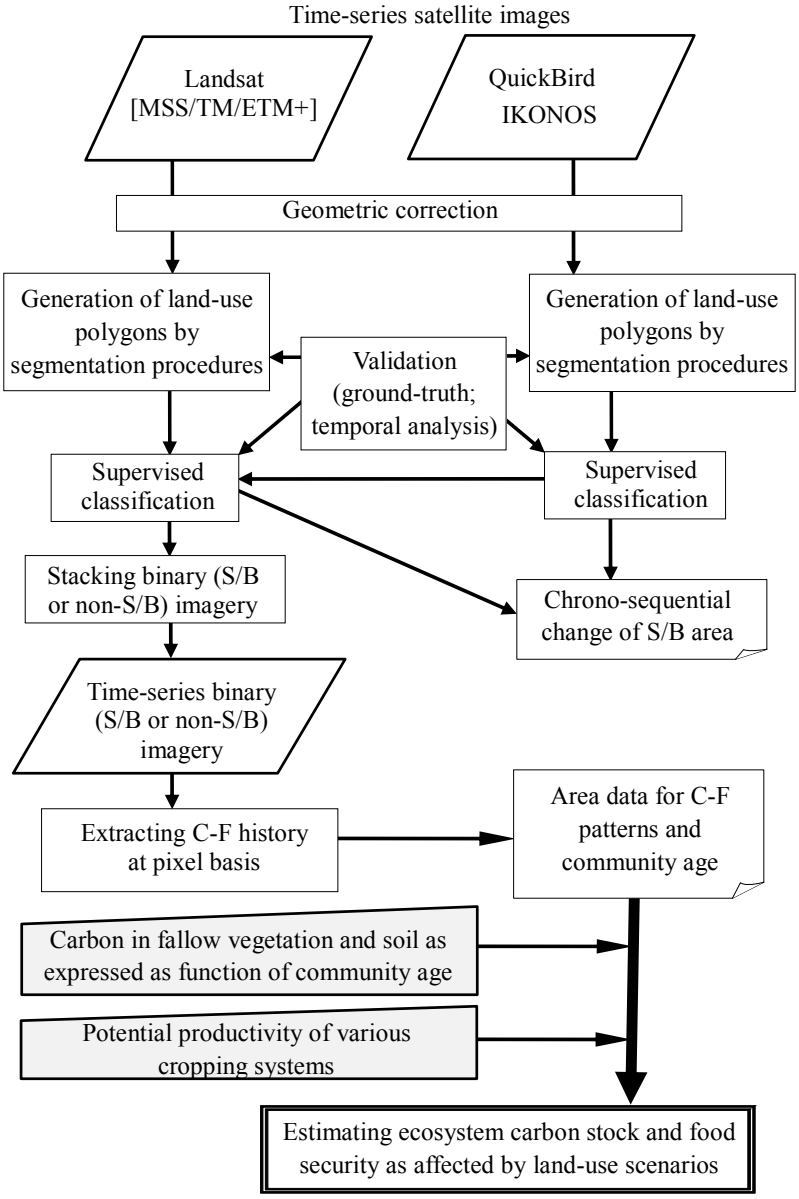

Fig. 9. A schematic diagram of satellite-image processing and assessment of land use and ecosystem carbon stock.

3.2.3 An approach to estimate ecosystem carbon stock at a regional scale

Direct quantification of biomass, height, or age using satellite optical signatures remains a challenging task for any types of remotely-sensed signatures even in simple tree stands (e.g. Foody et al., 2003; Dong et al., 2003; Franklin et al., 2003). Furthermore, the rapid recovery of tropical species, steep topography, and monsoon climate conditions in the tropical region add extra difficulties to such approach (Lambin et al., 1999; Inoue et al., 2007). Hence, we used the community age derived from the analysis of time-series satellite images as a clue to link the land-use patterns and *in situ* measurements for estimating the ecosystem carbon stock in the region. The analytical scheme is shown in Fig. 9. This approach is rather simple but no similar attempts have been reported before.

Regional ecosystem carbon stock C_R (MgC ha^{-1}) was estimated from the area A (ha), area ratio R_k (%) and ecosystem carbon stock C_{Ek} (MgC ha^{-1}) for each land-use pattern (C+F cycle) *k* using the following equations;

$$C_R = A\sum_k \left[0.01 R_k \cdot C_{Ek}\right] \quad (6)$$

$$C_E = C_V + C_S \quad (7),$$

where C_V (MgC ha^{-1}) is the carbon stock in crop or fallow vegetation including biomass, dead biomass, litter fall and roots, and C_S (MgC ha^{-1}) is the carbon stock in the soil at the depth of 0.3 m. The ecosystem carbon stock C_{Ek} in various C+F cycles (*k*) was estimated by combining simple semi-empirical models for C_V and C_S both of which were expressed as a function of community age. The R_k was estimated from the polygon-based classification of time-series satellite imagery as explained in the previous section. These partial models were derived respectively from the concurrent experimental studies on site. Details are reported in Kiyono et al. (2007) and Asai et al. (2007; 2009).

In brief, the sum of carbon stock C_V in the fallow vegetation (biomass, dead biomass, litter fall and roots) was estimated using an experimental equation derived from the data obtained by allometry method with complete tree tally (Kiyono et al., 2007);

$$C_V = 15.378 \ln(Y) + 11.815 \quad (8)$$

where Y is the community age. Measurements were made in the intensive study area once a year over 2002-2007 periods in six fixed plots with a range of community ages (0-20 yr). According to the model, the carbon in the fallow community was 12 and 47 MgC ha^{-1} one and ten years after abandonment, respectively. The applicability of the model was supported indirectly by the results on the relationship between community age and canopy height which is often used as a simple surrogate of C_V in a wider range of sites within the whole study area (Kiyono et al., 2007). Since no other data and equations have been available, we assumed this equation could represent the chrono-sequential change of C_V in the normal fallow vegetation in the region.

The carbon stock in the soil C_S was derived from *in situ* measurements of carbon exchange processes such as soil respiration, soil organic carbon and dry matter of roots (Asai et al., 2007; 2009). Carbon of crop biomass (heads, stems, and roots) was assessed by destructive sampling. Data were

collected in experimental fields in the Northern Agriculture and Forestry Research Centre (Houaykhot village) as well as the fixed fallow plots (0-20 yr) used for estimating C_V. It has been confirmed that range of measurements were comparable with previously reported values for tropical ecosystems (Tulaphitak et al., 1985; Bruun et al., 2006; Aumtong et al., 2009). These data were used to derive the parameters in a simple process model of carbon stock and flow in the soil such as decomposition rate and partitioning ratios of soil organic matter and litter (Nakane et al., 1983). Details of measurements and model derivation are found in these papers. Essential parts are summarized as follows.

$$dC_S = \tau_L D_L + \tau_{DR} D_R - k_t C_S \quad (9)$$

$$D_L = 4.85 / \{1 + \exp [-0.791 (Y-1.56)\} \quad (10)$$

$$D_R = 4.60 / \{1 + \exp [-0.340 (Y-1.59)\} \quad (11),$$

where dC_S is the annual increment of soil carbon, D_L and D_R are the carbon in the litter fall and fine root during fallow periods, τ_L and τ_{DR} are the partitioning rate of litter fall and fine root to soil carbon (0.14 and 0.72), k_t: turnover rate of soil carbon during cropping and fallow periods (0.17, 0.08), respectively. D_L and D_R during cropping periods were estimated to be 2.7 and 1.7 tC ha^{-1} based on sampling (Asai et al., 2007). We assumed that the above-ground fallow biomass would be lost after several times of burning practices, and the other parts as well as crop biomass left in the field would be decomposed based on the processes expressed in the above equations. The harvested crop parts were assumed to be consumed in a short term. The ratio of carbon in dry biomass is rather constant (47-50%) in each species (Asai et al. 2007; Kiyono et al., 2007). The effect of erosion was not taken into account since it may not be significant due to rapid recovery of vegetation coverage in S/B areas (Aumtong et al., 2009).

These experimental plots were carefully selected in typical area considering slope, aspects, elevation, vegetation and accessibility (Kiyono et al., 2007; Asai et al., 2007, 2009). The procedures to derive those semi-empirical models were conventional and model equations were fitted well to measured data. Nevertheless, due to constraints in logistics, the number of plots and thus the representativeness of the data and models are limited. Results have to be interpreted and utilized on the premise of the inherent uncertainty due to these limitations and assumptions. These semi-empirical models for C_V and C_S were synthesized, and linked with R_k by way of the community age derived from satellite image analysis in order to estimate the ecosystem carbon stock at a regional scale. This approach may provide new information for inferring the dynamics in regional ecosystem carbon stock as affected by land use.

3.2.4 Basis for scenario comparisons

Regional landscape consists of various land-use patches at a range of stages in C+F cycles. Therefore, in order to investigate the potential effects of land-use scenarios on the ecosystem carbon stock at a regional scale, we compared the regional average of ecosystem carbon stock under various

combinations of major C+F patterns. In the simulations hereafter, recent land-use situation (designated as scenario S1) was represented by the results in 2003 and 2004, and the total potential S/B area was assumed to be 67.4 % of the whole region derived from the analysis in 2003. Thus, each land-use scenario indicates how the potential S/B area (67.4 % of the whole region) is assigned to various C+F patterns and/or non S/B use. In other words, all scenarios were designed by altering some parts of the S1 scenario. In addition, some scenarios with alternative cropping systems (e.g., S4 and S5) and exclusion of 20 % of the S/B areas to conservation forest (e.g., S3 and S5) were examined. The alternative cropping scenarios assume a 2C+10F pattern enabled by new cropping technologies discussed later (section 4.5), while other scenarios assume traditional cropping practices. In the scenarios S3 and S5, 20 % of total potential S/B area (67.4 % of the whole study area) is reserved for conservation forest and never used for S/B. Details are explained in Sections 4.4.

On the other hand, we attempted to provide some reference information on the feasibility of such land-use scenarios in a viewpoint of merit for livelihood. The gross regional income was compared for some selected scenarios (S1-S5) based on preliminary simulation. Basic data and information for the simulation such as crop yield, prices of products, cost of input materials, labour cost, etc. were collected from the reconnaissance and the on-site experiments (Saito et al., 2006a; Asai et al., 2009). The rice yield was assumed to be 1.7 and 2.55 Mg ha^{-1} in indigenous and improved cultivars, respectively. Standard yield of paper mulberry 1.2 Mg ha^{-1} was used. Price of rough rice and bark of paper mulberry was 0.117 US$ kg^{-1} and 0.35 US$ kg^{-1}, whereas the cost for seedlings and seed for was negligible since they are native to the region. The values of annual labour for agricultural management (seeding, weeding, harvesting, etc.) and wages for the labour were assumed to be 278 man-days yr^{-1}, and 1.2 US$ d^{-1}, respectively. In all scenarios, no agro-chemicals were used as in the present situation. Fertilizer is not used in the region because fertilizer application has never been profitable. Possible income from carbon gain was not accounted in this calculation. Use of fossil fuels and machinery were not involved in these scenarios.

3.3 Results and discussion

3.3.1 S/B land use in the region

The recent status of major land-use types in the intensive study area (350 km^2; Luang Prabang Province) was analyzed using high resolution satellite imagery (QuickBird; October 23, 2003). Table 2 shows the detailed classification results for the study area in 2003, where the monitoring plots for *in situ* measurements were established. The major types of land use, i.e. S/B patches, fallow vegetation areas, conservation forests including spiritual forests, teak plantations, paddy/croplands, water bodies, and road/bare soil/houses were discriminated by supervised classification using ground-based survey. The classification results were validated by *in situ* observations and the interviews with villagers on in land-use history during the reconnaissance. The high spatial resolution of the image (0.6 m and 2.4 m panchromatic and multi-spectral images, respectively) also allowed direct identification of land-use conditions. Overall accuracy was about 90%, and producer's accuracy and user's accuracy for the S/B patches were as high as 100% and 86 %, respectively. Nevertheless, results suggest that accurate discrimination of fallow periods or even the differences between short-fallow, long-fallow and

conservation forest may be difficult even with high resolution imagery. The areas for S/B cropping, short fallow (1-3 years), and longer fallow patches in 2003 were 12.9 %, 34.8 %, and 19.6 %, respectively. Since the longest fallow periods identified by ground-based survey was 20 years in this classification, the total of these area 67.4 % may have experienced the S/B land use in the past two decades, and likely be used periodically for S/B in the future. Results suggest that the sum of these categories (tree-dominant biome), 97.7%, could potentially be the forest if no human disturbance is applied. The area of paddy and other permanent cropland was limited to the narrow flat areas along streams.

Table 2 Land use in the intensive study area (350 km^2; Luang Prabang Province) estimated from classification of high-resolution satellite image acquired on October 23, 2003 by a satellite QuickBird.

	Land use	Polygons	Area (ha)	Area (%)	Producer's accuracy (%)	User's accuracy (%)
1	Slash-and-burn (S/B)	4,031	3,952	12.9	100.0	86.0
2	Fallow [1-3 years] (FS)	5,348	10,656	34.8	91.3	80.8
3	Fallow [4< years] (FL)	3,467	6,010	19.6	63.6	70.0
4	Consevation Forest (CF)	4,704	7,759	25.4	83.3	70.0
5	Teak plantation	824	1,515	5.0	62.5	71.4
6	Paddy/Other cropland	177	202	0.7	83.3	90.9
7	Water (river/pond)	85	174	0.6	100.0	100.0
8	Road/Bare soil/House	603	326	1.1	81.8	100.0
	Total	19,239	30,595	100.0	Overall accuracy = 89.5%	
	SB + FS + FL	12,846	20,618	67.4	Kappa = 0.878	
	SB+FS+FL+CF+Teak [potential forest area]	18,374	29,892	97.7		

Notes: 'Producer's accuracy' means the ratio of the number of correctly-classified pixels of a certain category against the true sum of pixels of that category. User's accuracy is the ratio of the number of correctly-classified pixels of a certain category against the total number of pixels that were classified in that category. Hence, 'Producer's accuracy' is a measure of omission error while 'User's accuracy' is of commission error.

In order to derive the temporal change of land use, the S/B cropping patches in each year was derived from individual Landsat satellite image based on the polygon-based classification procedures over 1973-2005 periods. Table 3 shows the classification accuracy in some satellite images that were validated using the ground-based truth data and high resolution satellite images. Both producer's and user's accuracy for discrimination of S/B patches were higher than 0.95. Figure 10 shows the frequency distribution of the size of S/B cropping patches in 2003 derived from Landsat ETM+ image for three different areas in Luang Prabang province (Houaykhot, Muang Ngoy, and Pakmong). Obviously, the distribution patterns for the three areas were quite similar, so that these results suggest the size frequency of management unit for S/B cropping in the province. Overall, the patch size around

0.6-1.2 ha was the majority (38 ± 2 %), and 83 ± 3 % were smaller than 2 ha, whereas only 5 ± 2 % were larger than 3 ha. Since polygons were created based on spectral similarity and continuity of boundary, these patch size may not always be equivalent to those of management unit linked to ownership, but regional tendency can be inferred from the distribution. For example, 95 % the patches were smaller than 1.2 ha in Oudomxay, whereas 38 % were larger than 3 ha in Muang Houn, respectively. These differences may be related to local variability in indigenous management practices, ownership system, family structure, and ethnic traditions.

Table 3 Accuracy in distinguishing slash-and-burn patches using segmentation-based classification with Landsat spectral bands.

Date yyyymmdd	Producer's accuracy for S/B (%)	User's accuracy for S/B (%)	Overall accuracy (%)
19991116	98.0	100.0	80.2
20001102	100.0	94.1	85.9
20011121	100.0	100.0	79.2
20021108	95.7	100.0	85.1
20031205	100.0	96.0	76.0
20041207	98.0	97.0	86.2
20051124	99.0	95.5	84.5
Average	98.7	97.5	82.4

Notes: Definitions of 'accuracies' are same as in Table 2. Training samples consisted of 20 S/B patches in each year.

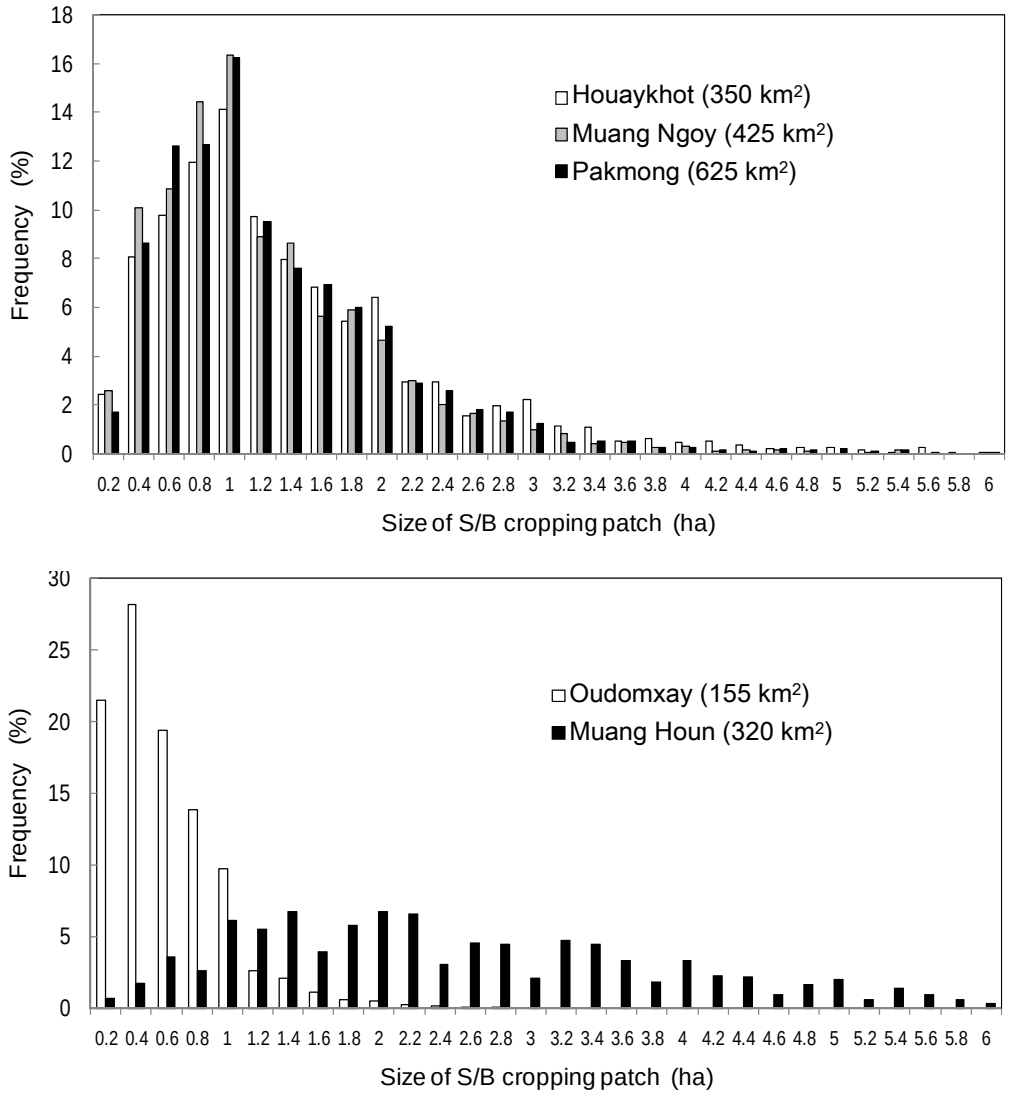

Fig. 10. Frequency distribution of size of S/B cropping patches in the intensive study areas in Luang Prabang province in 2003. Results are derived from polygon-based classification of Landsat ETM+ image acquired on December 5, 2003.

Figure 11 shows the temporal change of the S/B cropping area in the intensive study area. The cropping area by S/B practice in each year increased rapidly from around 5 % in 1970's to 12 % in 2000s. The increase during 1990s was remarkable, while it was still small before mid-1980s. The annual increment rate during the decade after 1990 was about 3.8 % for the study area. Similar analysis conducted in several other areas within the whole study area showed the annual rate of 3-5 % for the decade. Although the recent trend suggests somewhat slowing down, yet, no decreasing trend has been found during the period of analysis. These estimates support the descriptive information from reconnaissances at various sites in the region (e.g. Roder, 2001; Douangsavanh et al., 2006).

3.3.2 Community age of fallow vegetation

The multi-layered binary (S/B and non-S/B) dataset generated from the consecutive satellite images allowed systematic analysis of chrono-sequential patterns of land use at the resolution of satellite sensor pixels (30 m). The S/B or non-S/B land-use history could be traced at a pixel basis for the area of interest, so that the important land-use parameters such as duration of consecutive cropping period or community age of fallow vegetation were derived systematically from the dataset. This was the most crucial role of time-series satellite images in this analysis although few reports on similar approach are found.

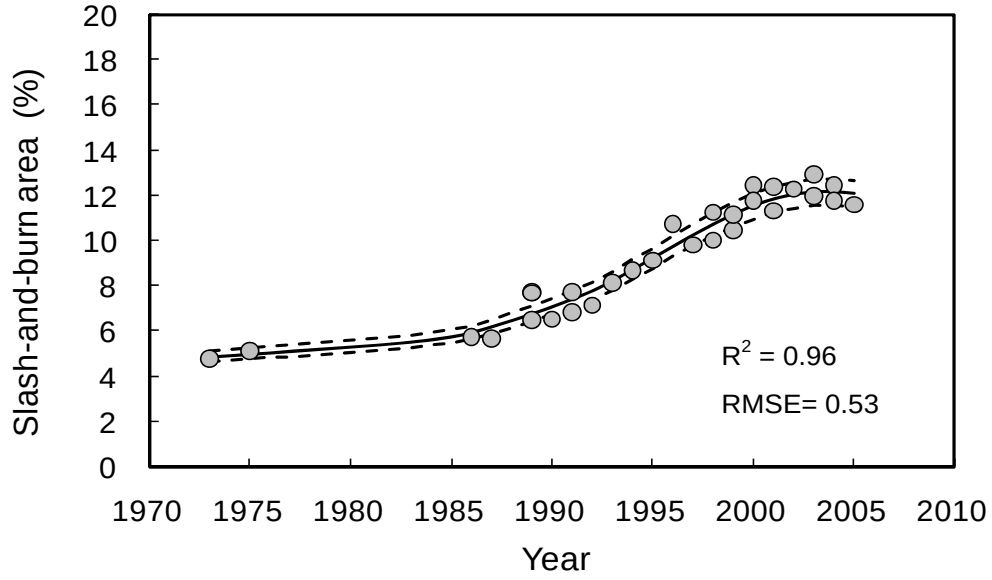

Fig. 11. Temporal change of slash-and-burn cropping area in each year in the intensive study area (350 km^2) in Luang Prabang province. A smoothing-spline curve was fitted, for which the dotted lines indicate ±5 % range.

First, we examined the land-use intensity in the region by tracing the consecutive S/B use. Figure 12 shows the relative area (%) of consecutive S/B cropping periods (yr) among the total S/B cropped area in each year. The "1 yr" means that a pixel was newly used for S/B in the year, and "2 yr" indicates the second year of S/B use, and so forth. Some parts of "1 yr" pixels are to be used in the next year again for S/B, so counted as "2 yr", accordingly. For the period from 1993 to 2005, the average (± standard deviation) for 1, 2, and 3 y was 74.7 ± 6.8 %, 18 ± 5.2 %, and 4.6 ± 1.8 %, respectively. Results suggest that the relative ratio of consecutive S/B periods is rather stable even though the total S/B area has been changing as shown in Fig. 11. On average, 75 % of S/B area in each year was newly slashed patches, 76 % out of which is abandoned after a single year of cropping. Long S/B consecutive use (>4 yr) is very minor in the region. These estimates agree the descriptive information and experimental results that suggest the trend in the regional land use and the drastic decrease in crop yield during consecutive cropping (e.g. Roder, 2001; Douangsavanh et al., 2006; Saito et al., 2006a; Asai et al., 2009).

Next, we examined the fallow length in the region. Community age of fallow vegetation can be calculated at a pixel basis by tracing back to the last S/B use on each pixel. Area distribution (%) of each community age in the whole area was derived in 2003 and 2004, respectively, and their average was used to represent the recent land use (Fig. 13a). The graph shows that the area for age = 0 (S/B) was largest (11.24 % of the whole area) whereas the area for community age of 1-3 yr was 28%, and 50 % for 1-12 yr, respectively. These values proved comparable with the classification results using the high resolution imagery (Table 2), although some uncertainty remains since the community age larger than 13 years could not be traced due to missing year in time-series Landsat imagery. Since no other information on community age was available, we used the result of community age in 2003-2004 (Fig. 13a) for comparative analysis of land-use scenarios, assuming it is representative of the recent land-use condition in the region.

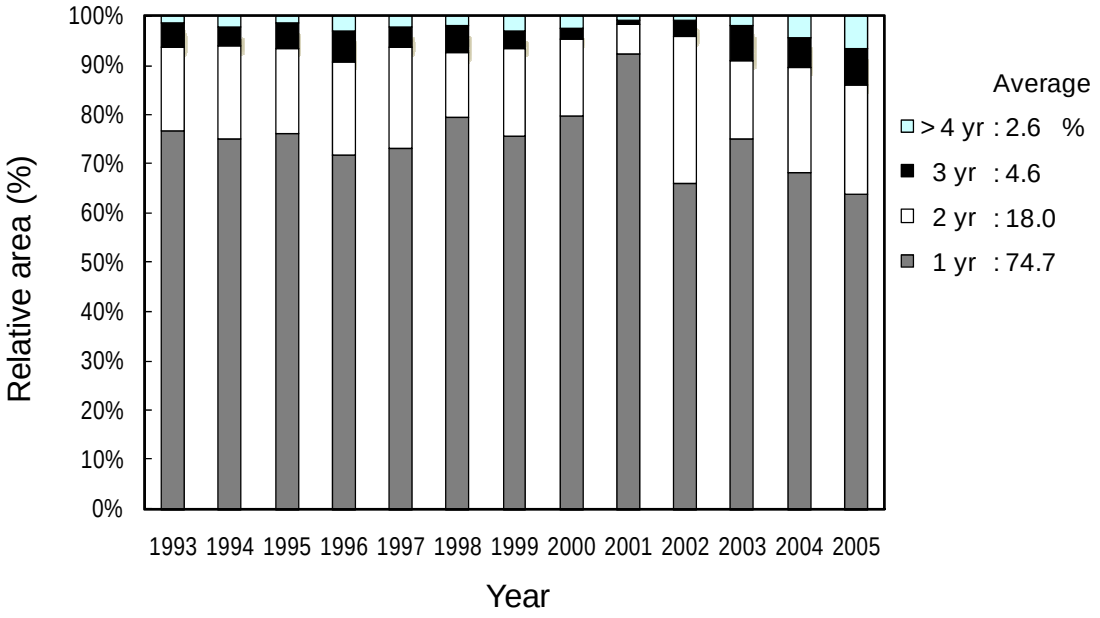

Fig. 12. Relative area of consecutive S/B land use among the S/B cropping area in each year.

From Fig. 13a, we estimated the recent situation of S/B land-use patterns, i.e. the fallow length in the study area in case this situation would continue. The differential between the areas of consecutive community ages was assumed to be the area that was converted to cropping after the specific fallow length. In general, the differential (CA_i - CA_{i+1}) of the areas in two consecutive community ages (CA at i and i+1 years) indicates the area that was converted to S/B cropping after i year-fallow period. For example, the differential area between the community ages 4 yr and 3 yr implies that this differential area has been converted to S/B cropping after 3 yr fallow period. In other words, if the differential is zero (area for 3 yr = area for 4 yr), all of 3 yr fallow vegetation remained undisturbed to grow to age 4 yr in the next year. We applied this approach to the average values for the 2003-2004 assuming the change was small during the period. Accordingly, Figure 13b shows the relative area for each fallow length in 2003-2004 periods. The most common fallow length was 3 yr (20%) followed by 2 yr (17.5 %), that is, the major C+F cycle is 1 yr cropping - 3 yr fallow (1C+3F) pattern followed by 1C+2F pattern. The area for short fallow (1-3F yr) was up to 45 %, while the area

for 5-11 yr fallow was 27 %. It was also confirmed that long-fallow areas (>11 y) are still used in part (9 %) for S/B cropping. These findings agreed well with the general information from ground-based reconnaissance, which also support the qualitative descriptions on overall trend of S/B land use in the region (Fujisaka, 1991; Roder, 2001; Pravongvienkham, 2004). General trends in S/B land use have been reported based on observations, but these results may be the first of this kind based on chrono-sequential analysis of time-series satellite imagery. It is obvious that we have to be careful about the possible errors in data and analytical procedures as well as the representativeness, but results may be useful to infer the comprehensive land-use conditions at a regional scale. When the time-series satellite images are available over extended periods, the same approach would provide more useful information on the dynamic land-use history.

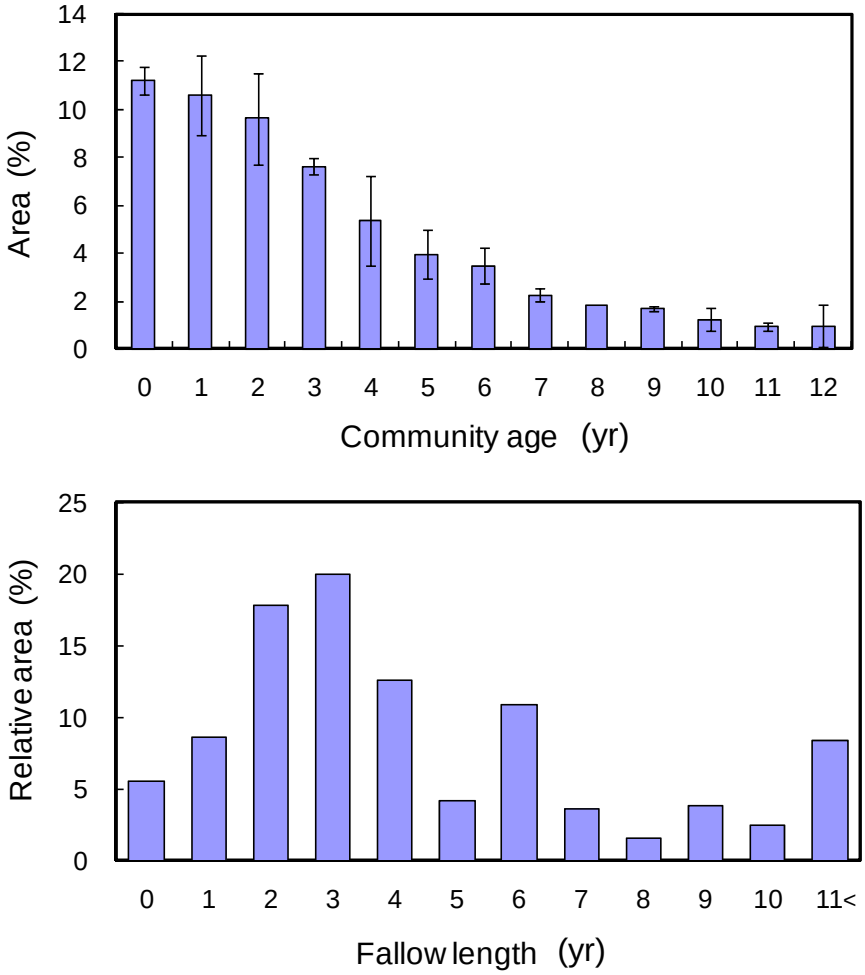

Fig. 13. Areas for each community age of fallow vegetation within the whole region (a), and relative areas for different fallow lengths (b) during 2003-2004 periods.

3.3.3 Chrono-sequential change of ecosystem carbon stock in various land-use patterns

The chrono-sequential change of ecosystem carbon stock was simulated under various combinations of C+F patterns based on the approach described in section 2.4. Since the region has been under S/B land use long time, effects of repeated land-use cycles were not taken into account explicitly in this

approach assuming that such effects are included in each partial model. Figure 14 shows the chrono-sequential change of ecosystem carbon stock under some typical C+F cycles. The initial value was set to be a typical value measured just before cropping (42.0 Mg ha^{-1}) estimated from in *situ* measurements (Asai et al., 2007), which is comparable with the reported range (Bruun et al., 2006). Obviously, the major increase in ecosystem carbon stock is brought by biomass growth of fallow vegetation (secondary forest), while the drastic drop is caused by S/B practice. Even within the selected C+F patterns, the average value over 35 years varied up to 33 MgC ha^{-1}. In case of 1C+3F pattern (i.e. a cycle of 1-yr cropping with 3-yr fallow), the temporal average during 35 years was 41.7 MgC ha^{-1}, which is nearly the same as the initial values, but in the 1C+2F cycle, the temporal average 34.9 MgC ha^{-1} was lower than the initial carbon level by 7.1 MgC ha^{-1}. For example, the temporal

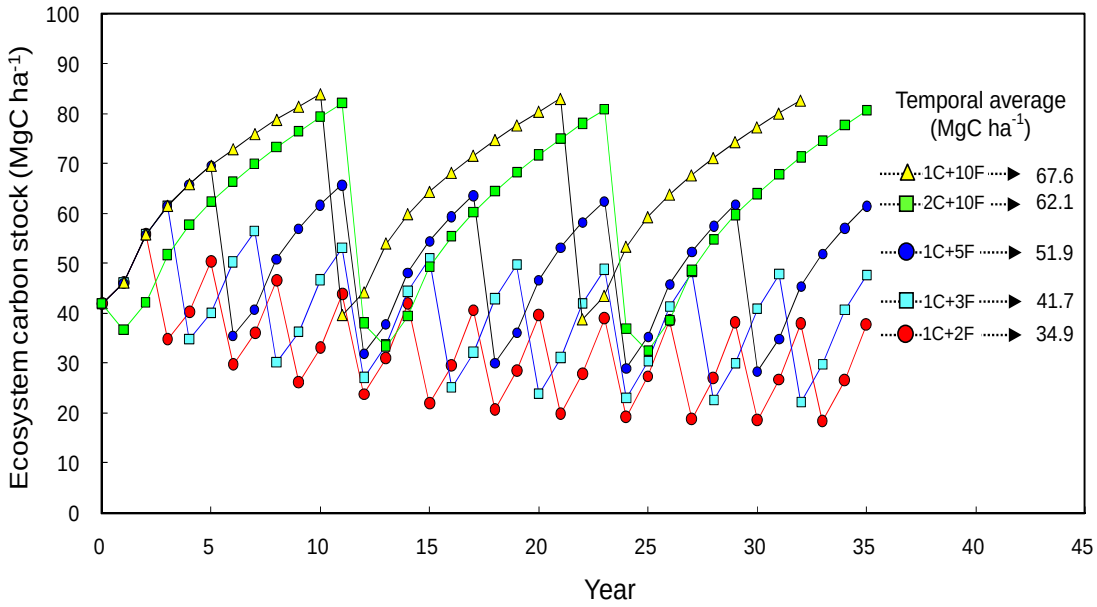

Fig. 14. Chrono-sequential changes in ecosystem carbon stock under some typical land-use patterns as assessed by a coupled model of carbon in the soil and fallow vegetation. "C" and "F" denote cropping and fallow, respectively, so that "1C+10F", e.g., means 1-yr cropping and 10-yr fallow pattern. The arrow and number attached to each line indicate the temporal average of carbon stock.

average of carbon stock in 2C+10F cycle was larger than that in 1C+3F by 21 MgC ha^{-1}, which suggests that this amount could be sequestrated into the ecosystem from the atmosphere by changing the land-use pattern from 1C+3F to 2C+10F. The bottom points in each line indicate the carbon level just after S/B practice. The decreasing trend was obvious in short fallow patterns, but also some slight decreasing trend was still found even under the 10 yr fallow patterns (e.g. 1C+10F). There might be some more complex C-F combinations, but according to our field observation, interview with villagers, and historical records (e.g., Fujisaka, 1991; Roder, 2001) as well as satellite image analysis, the major C-F combinations are quite simple. Hence, we assumed that simple C-F combinations would sufficiently represent the real situation in the region. In this assessment, the same carbon model was applied during the repeated C+F cycles assuming that the plant growth was not affected by the level of soil carbon. However, a positive correlation found between soil carbon content and rice yield at the

study site (Asai et al., 2009) suggests that the vegetation growth may be lower than the model estimates due to decreased level of soil carbon. Although there are few quantitative analyses on long-term effects of repeated short-fallow cycles, some villages have already given up continuing the S/B land use due to the serious decrease in crop yield. Therefore, it may not be possible to repeat such short-fallow cycles as 1C+2F for long term as simulated in Fig. 14. There might be another serious story that natural succession processes from the poor herbaceous vegetation to forest biome might not occur after such degraded conditions (Gomets-Pompa et al, 1972).

The model-based assessment of ecosystem carbon stock was reasonable compared to the above-ground carbon in mature tropical forests under similar climatic conditions (Vargas et al., 2008). In this relative comparison, some part of uncertainty due to limitations in the availability of *in situ* data and simplifications in modelling procedures may be cancelled. No data are available to estimate the absolute error in the long term average, but it may be in the order of ±3.6 and 6.2 MgC ha^{-1} in 1C+2F and 1C+10F cycles, respectively if the uncertainty due to modelling and representativeness is ±10 %. Results may be useful to infer the impact of land use on the ecosystem carbon stock and the potential of carbon sequestration by changing land-use and ecosystem management practices.

3.3.4 Comparison of regional carbon stock under various land-use scenarios

As examined in section 3.2, a region consists of various land-use patches at a range of stages in C+F cycles. Therefore, we compared the regional average of ecosystem carbon stock under various combinations of major C+F patterns.

The graph in Fig. 15 depicts the regional average of ecosystem carbon stock under some selected scenarios. The upper part of the table attached to Fig. 15 shows the percentage areas for the dominant combinations of C+F patterns in each land-use scenario. Land-use scenarios in 1980 and 1990 are also included for reference using the area data (Fig. 11) and most probable S/B patterns inferred from interview during the reconnaissance and previous studies (Fujisaka, 1991; Roder, 2001). It is obvious that the regional average of carbon stock increases by elongating the minimum fallow length as in S4 scenario compared to the present status (S1). On the other hand, regional carbon stock decreases by reducing the longer fallow periods as in S2; however, the change is rather small partly because the areas with long-fallow patterns have already been reduced considerably in the present situation, and because the growth rate of fallow vegetation is lower for higher community age. The ecosystem carbon stock will increase by 10.5 MgC ha^{-1} if the 1C+5F pattern and those with shorter fallow are all replaced with 1C+6F, whereas it will decrease by 8.8 MgC ha^{-1} if longer fallow are diminished leaving 1C+3F or shorter fallow patterns. The exclusion of 20 % area from S/B land use to conservation forest (S3 and S5) is also effective to increase the regional carbon stock since the area is never used again for S/B in the future. The increase of S3 from S1 was 9.1 MgC ha^{-1}.

The difference of carbon stock in 1980 and 1990 scenarios was small as presumed from the slow rate of area change in Fig. 11, but the differential from 1990 to the recent status (S1: 2003/2004) was as large as 41.6 MgC $ha^{-1}$for the ecosystems in the region. This change is caused partly by the increase in S/B area and partly by the shortened fallow periods; the former effect is quantified in Fig. 11, and the latter effect is quantified in Fig. 15. This value may be a hypothetic basis to infer the amount of

carbon released from the ecosystems in the tropical mountain to the atmosphere during the period. There are no similar data for the region to be compared; however, Houghton and Hackler (1999) and Flint and Richards (1994) have reported that the change in average forest biomass in tropical Asia between 1880 and 1980 was 23 MgC ha^{-1} and 43 MgC ha^{-1}, respectively. Although these estimates are for a 100 year period, our estimates may be comparable with these values because the major change in the study area has occurred after the late 1980s as indicated in Fig. 11. It is reasonable to assume a little change during the first half of the 100 years and drastic changes during the second half occurred in the region (Fujisaka, 1991; Roder, 2001).

3.3.5 Implications of land-use scenarios to livelihood

The major focuses in this study are regional land use and ecosystem carbon stock, as well as the possible influence of land-use scenarios on regional carbon stock. Nevertheless, food and resource security (sustainability of forest, NTFP, drinking water, biodiversity) is of the highest priority for livelihood in the region (Rasul and Gopal, 2003; Douangsavanh et al., 2006). In other words, the global carbon issue receives little attention at the moment and carbon sequestration cannot be any incentive for changing regional land use. There are some evidences showing that shorter fallow period is associated, more or less, with some negative effects on crop yield, non-timber forest products, and labour productivity (Tulaphitak et al., 1985, Fujisaka, 1991; Roder, 2001; Bruun et al., 2006; Saito et al., 2006a, b; Jakobsen et al., 2007). Due to decreasing land and labour productivities, villagers are forced to expand the S/B area illegally to the long-fallow or conservation areas. During the field reconnaissance in 2006-2007, S/B practices at long-fallow or conservation forest areas (community age > 15 yr) have been sometimes observed. The conflict between forest conservation and the livelihoods of poor people seemed serious. One of different options for them after complete land degradation is to work as labourers in rubber plantations. Nevertheless, it was obvious that such commercial plantations were carefully limited to narrow areas with easy access along the roads due to new policies implemented by the government (Fujita and Phanvilay, 2008). Hence, the majority of S/B region may suffer similar problems sooner or later. Therefore, alternative land-use scenarios are strongly required for higher food and resource security as well as for higher carbon stock. The balancing between food production and environmental remediation is of increasing importance in ecosystem management and policy making, especially in developing countries (Smith et al., 1999; Pravongvienkham, 2004; Grau et al., 2008).

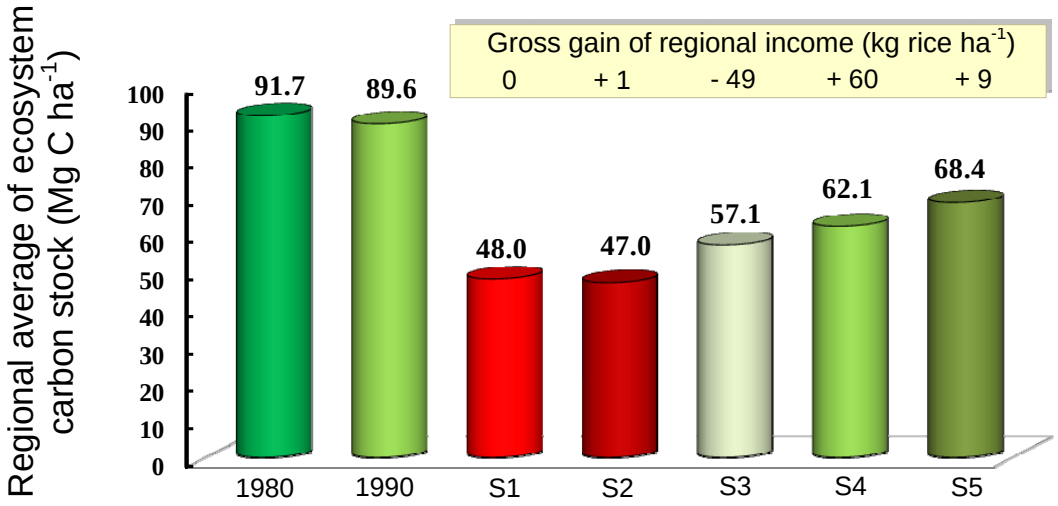

	Scenarios	1980	1990	S1	S2	S3	S4	S5
	Summary of land-use and ecosystem management	Estimated S/B area & land-use patterns in 1980.	Estimated S/B area & land-use patterns in 1990.	Same S/B area & land-use patterns as in 2003/2004.	Same S/B area as 1, but limit longest fallow to 8 yr.	Reserve 20% for conservation forest, but same land-use pattern as 1.	Same S/B area as 1, but adopt alternative 12 yr cycle land-use management.	Reserve 20% for conservation forest & adopt alternative 12 yr cycle management.
Area ratio for S/B land-use cycles (%)	1C+1F	0	0	8.6	8.6	6.9	0	0
	1C+2F	0	0	17.9	17.9	14.3	0	0
	1C+3F	0	0.0	20.0	20.0	16.0	0	0
	1C+4F	0	0.0	12.6	12.6	10.1	0	0
	1C+5F	0	7.6	4.3	4.3	3.4	0	0
	1C+6F	0	1.1	11.0	11.0	8.8	0	0
	1C+7F	0	0.3	3.6	3.6	2.9	0	0
	1C+8F	0	0.1	1.6	22.1	1.3	0	0
	1C+9F	6.4	0.3	3.9	0	3.1	0	0
	1C+10F	0.2	0.2	2.5	0	2.0	0	0
	1C+11F	0.7	0.5	8.5	0	6.8	0	0
	2C+11F	0.4	0.3	5.6	0	4.5	0	0
	2C+10F	-	-	-	-	-	100.0	80.0
	1C+no use	91.7	89.6	-	-	20.0	-	20.0
Gross regional income	Rice production							
	Indigenous cultivars	-	-	261.8	262.8	157.1	-	-
	Improved cultivars	-	-	-	-	-	286.1	228.8
	Cash crop (paper mulberry)	-	-	0.0	0.0	0.0	112.2	89.7
	Technical cost							
	Seed: indigenous	-	-	-11.5	-11.6	-6.9	-	-
	Seed; improved cultivar	-	-	-	-	-	-19.6	-15.7
	Technology transfer	-	-	0.0	0.0	0.0	-75.0	-75.0
	Income from surplus labor	-	-	0.0	0.0	51.4	6.8	31.1
	Total balance (kg rice ha^{-1})	-	-	250.2	251.2	201.5	310.4	259.0

Note: Gross regional income was derived as the sum of balance for all land-use patterns within the S/B areas.
All figures are expressed in the amount of rice (kg) of their equivalent value.

Fig. 15. Comparison of regional carbon stock and gross regional income under a few selected land use and ecosystem management scenarios based ona simulation for 35 years. Tables show the percentage areas of dominant copping (C) and fallow (F) periods for each land-use scenarios.

Against this background, alternative cropping systems for higher rice productivity and/or improved income have been investigated in the study area concurrently with the present study (Saito et al., 2006a, b; Asai et al., 2009). High yielding rice cultivars, green manure plants and cash crops have been screened to evaluate their performance under S/B conditions. These studies suggested that the cropping system based on the combination of high yielding rice cultivars, green manure plants (e.g. *Stylosanthes guianensis*) and cash crop (e.g. paper mulberry) is most promising, and that the system would allow 2C+10F pattern (Asai et al., 2007). Hence, we included the S4 and S5 scenarios in Fig. 15, i.e. 2C+10F land-use pattern using this new cropping system. The simulation in Fig. 15 suggests that S4 and S5 would allow some significant increase in regional carbon stock (14.1 and 20.4 MgC ha^{-1}, respectively).

On the basis of these background and investigations, we attempted to provide some reference information on the adoption potential of various land-use scenarios. The gross regional income was compared for the selected scenarios based on preliminary simulation (The lower part of the table in Fig. 15). The gross gain of regional income in S2 is estimated to be comparable with S1, while the ecosystem carbon stock is lowered by 1.0 Mg ha^{-1}. In S3 scenario, a relatively large increase of carbon level is expected, but the income is seriously reduced. If the possible crop-yield reduction due to repeated short fallow cycles was included, results may be worse in reality under short fallow scenarios (e.g. S1 and S2). The S4 scenario allows the highest gain in gross income as well as relatively high carbon level, but the total area of S/B is not reduced. In the S5 scenario, the increase in carbon level is highest, while the gross income is also improved to some extent. Hence, some reasonable scenarios for balancing food security and carbon sequestration may exist between S4 and S5 scenarios. These simulations are based on the most probable data and information at the moment, but should be affected by many conditions such market price of products. Nevertheless, results may help designing the regional land-use and ecosystem management scenarios taking account of both gross regional benefit and carbon stock capacity of the region. In this simulation, we assumed a simple alternative land-use such as S4, but further agronomic studies in the area will add a wider range of cropping options for new alternative scenarios. Carbon trading was not included in this preliminary investigation, but it may add a positive incentive towards improved ecosystem management.

3.4 Summary

This study was conducted to provide the quantitative basis to better understand and manage the land use and ecosystem carbon stock in the slash-and-burn region of tropical mountains in Laos.

The use of time-series satellite images proved useful to derive not only the chrono-sequential change of land use, but also the relative areas for consecutive S/B use, community age, and C+F patterns. The cropping area by S/B practice in each year increased rapidly from around 5 % in 1970's to 12 % in 2000s; especially, the increase during 1990s was remarkable, while it was still small before mid-1980s. The annual increasing rate of S/B cropping area during the decade after 1990 was estimated to be 3-5 % in the northern part of Laos. In 2003, the total potential area for S/B land use was estimated to be up to 60-70 % of the whole area. On average, 75 % of S/B area in each year were newly slashed patches, whereas nearly the same area (76%) was abandoned after a single year of

cropping. Long S/B consecutive use (>4 yr) was very minor. Approximately 37 % of the whole area was with the community age of 1-5 years, whereas 10 % for 6-10 years. The most common fallow length was 3 yr (20% of cropped area by S/B) followed by 2 yr (17.5 %). The ratio of short fallow (1-3 yr) was up to 45 %, while the ratio of 5-11 yr fallow was 27 %. It was also found that long-fallow areas (>11 yr) were slashed and burnt for cropping (9 %).

These data played a crucial role in the regional assessment of ecosystem carbon stock through the combination with semi-empirical model derived from *in situ* measurements. A large variability was found in the temporal average of carbon stock under various C+F patterns; e.g. 33 MgC ha^{-1} between 1C+2F and 1C+10F cycles. Simulation results on the average ecosystem carbon stock in the potential S/B area under various land-use scenarios suggested strong effects of land-use and ecosystem management on the regional carbon stock. Under the land-use situation in recent years (2003-2004), the average carbon stock would increase by 10.5 MgC ha^{-1} if the 1C+5F pattern and those with shorter fallow were all replaced with 1C+6F, whereas it would decrease by 8.8 MgC ha^{-1} if longer fallow periods were diminished leaving 1C+3F or shorter fallow patterns. The differential from 1990 to the recent status was inferred to be 41.6 MgC ha^{-1}. This large change was caused by the increased S/B area and by the shortened fallow periods.

Poverty is a serious problem in the region and food security is the highest priority for villagers, while livelihood depends largely on the S/B land use. Considering the recent situation observed during reconnaissance, people are forced to expand the S/B area illegally into the long-fallow or conservation areas due to decreasing land- and labour-productivities. Therefore, alternative land-use scenarios should be beneficial to regional livelihood. Preliminary accounting suggested that alternative scenarios with prolonged fallow periods (such as 2C+10F) in support of new cropping systems may contribute both higher food security and carbon sequestration. Carbon trading was not included in the preliminary accounting, but it could add a positive incentive to push the national and international efforts towards poverty reduction through alteration of regional land-use and ecosystem management (Perez et al., 2007).

Results would be useful to design more productive and sustainable land-use and ecosystem management scenarios taking account of the carbon-sequestration capacity and benefit to regional livelihood. This study demonstrated the unique potential of synergistic use of *in situ* measurements, modelling and satellite data, especially in such regions with the limitations in data availability and accessibility. Nevertheless, the applicability of the methods and the present results to wider regions should be examined in various sites. Further research efforts should also be dedicated to the assessment and adoption strategies of promising ecosystem-management scenarios. International and interdisciplinary collaborations are crucial for solving these regional agro-environmental problems.

4. Conclusions - role of remote sensing in soil carbon applications -

The present case studies showed a few aspects of the wide range of potential applications of remote sensing in soil and ecosystem carbon applications. The major role of remote sensing in these applications is to quantify the chrono-sequential change of the following key-variables/conditions at various scales;

1) Land-use --- forest, grassland, crop land, degraded land, urban, park, etc. Transformation between these land-use categories would have the major impacts on the regional carbon stock.

2) Land-cover --- surface conditions: vegetation, water, soil, impervious structure, etc. The surface conditions have strong influence on carbon flux of ecosystems.

3) Management practices --- tillage/non-tillage, planting, harvesting, irrigation, residue, etc. Method, intensity and timing of these practices would have some effects on the ecosystem carbon stock as operational options for mitigation in the field.

4) Soil properties --- soil color, soil carbon, water, etc. This may be the most direct application of remote sensing to the soil.

A great deal of remote sensing data including hyperspectral and microwave signatures are to be obtained by advanced satellite sensors (Pearlman et al., 2003). Further systematic efforts are needed for operational applications.

5. Acknowledgements

This paper was written based on several collaborative studies with a number of domestic and international collaborators including Drs. Kiyono, Y., Ochiai, Y., Asai, H., Horie, T., Saito, K., Shiraiwa, T., Qi, J., Olioso, A., Douangsavanh, L. and Zhi, X.

6. References

Asai, H., Saito, K., Samson, B., Vongmixay, K., Kiyono, Y., Inoue, Y., Shiraiwa, T., Homma, K., Horie, T., 2007. Quantification of soil organic carbon dynamics and assessment of upland rice productivity under the shifting cultivation systems in northern Laos. Proc. 2nd International Conference on Rice for the Future, November 5-9 2007, Bangkok, Thailand, pp.2001-205.

Asai, H., Saito, K., Samson, B.K., Songyikhangsuthor, K., Homma, K., Shiraiwa, T., Kiyono, Y., Inoue, Y., Horie, T., 2009. Yield response of indica and tropical japonica genotypes to soil fertility conditions under rainfed uplands in northern Laos. Field Crops Research 112, 141-148.

Aumtong, A., Magid, J., Bruun, S., de Neergaard, A., 2009. Relating soil carbon fractions to land use in sloping uplands in northern Thailand. Agriculture, Ecosystems and Environment 131, 229-239.

Bellamy, P.H., Loveland, P.J., Bradley, R.I., Lark, R.M., Kirk, G.J.D., 2005. Carbon losses from all soils across England and Wales 1978-2003. Nature 437, 245-248.

Ben-Dor, E., Taylor, R.G., Hill, J., Dematte, J.A.M., Whiting, M.L., Chabrillat, S., Sommer, S. 2008. Imaging spectrometry for soil applications. Advances in Agronomy, 97, 321-392.

Bruun, T.B., Mertz, O., Elberling, B., 2006. Linking yields of upland rice in shifting cultivation to fallow length and soil properties. Agriculture, Ecosystems and Environment 113, 139-149.

Cochrane, M.A., Alencar, A., Schulze, M.D., Souza, Jr. C.M., Nepstad, D.C., Lefebvre, P., Davidson, E.A., 1999. Positive feedbacks in the fire dynamic of closed canopy tropical rain forests. Science 284, 1832-1835.

Davidson, E.A., de Abreu Sá, T.D., Carvalho, C.J.R., de Oliveira Figueiredo, R., do Socorro, A., Kato, M., 2008. An integrated greenhouse gas assessment of an alternative to slash-and-burn agriculture in eastern Amazonia. Global Change Biology 14, 998-1007.

Dong, J., Kaufmann, R.K., Myneni, R.B., Tucker, C.J., Kauppi, P.E., Liski, J., Buermann, W., Alexeyev, V., Hughes, M.K., 2003. Remote sensing estimates of boreal and temperate forest woody biomass: carbon pools, sources, and sinks. Remote Sensing of Environment 84, 393-410.

Dorigo, W.A., Zurita-Milla, R., de Wit, A.J.W., Brazile, J., Singh, R., Schaepman, M.E., 2007. A review on reflective remote sensing and data assimilation techniques for enhanced agroecosystem modeling, International Journal of Applied Earth Observation and Geoinformation 9, 165-193.

Douangsavanh, L., Polthanee, A., Katawatin, R., 2006. Food security of shifting cultivation systems: Case Studies from Luang Prabang and Oudomxay Provinces, Lao PDR. Journal of Mountain Science 3, 48-57.

Dymond, J.R., Bégue, A., Loseen, D., 2001. Monitoring land at regional and national scales and the role of remote sensing, International Journal of Applied Earth Observation and Geoinformation 3, 162-175.

Flint, E.P., Richards, J.F., 1994. Trends in carbon content of vegetation in south and southeast Asia associated with changes in land use. In: Dale, V.H. (Ed.), Effects of Land Use Change on Atmospheric CO2 Concentrations: South and Southeast Asia as a Case Study, Springer, New York, pp. 201-299.

Foody, G.M., Boyd, D.S., Cutler, M.E.J., 2003. Predictive relations of tropical forest biomass from Landsat TM data and their transferability between regions. Remote Sensing of Environment 85, 463-474.

Franklin, S.E., Hall, R.J., Smith, L., Gerylo, G.R., 2003. Discrimination of conifer height, age and crown closure classes using Landsat-5 TM imagery in the Canadian Northwest Territories. International Journal of Remote Sensing 24, 1823-1834.

Fujisaka, S., 1991. diagnostic survey of shifting cultivation in northern Laos: targeting research to improve sustainability and productivity. Agroforestry Systems 13, 95-109.

Fujita, Y., Phanvilay, K., 2008. Land and forest allocation in Lao People's Democratic Republic: Comparison of case studies from community-based natural resource management research. Society and Natural Resources 21, 120–133.

Fung, I.Y., Doney, S.C., Lindsay, K., John, J., 2007. Evolution of carbon sinks in a changing climate. Proceedings of the National Academy of Science 102, 11201-11206.

Gomets-Pompa A., Vasquez-Yanes C., Guevara, S., 1972. The tropical rainforest: non-renewable resource. Science 177, 762-765.

Grau, H.R., Gasparri, N.I., Aide, T.M. 2008. Balancing food production and nature conservation in the Neotropical dry forests of northern Argentina. Global Change Biology 14, 985-997.

Hese, S., Lucht, W., Schmullius, C., Barnsley, M., Dubayah, R. Knorr, D., Neumann, K., Riedel, T., Schröter, K., 2005. Global biomass mapping for an improved understanding of the CO_2 balance - the Earth observation mission Carbon-3D. Remote Sensing of Environment 94, 94-104.

Hirsch, A.I., Little, W.S., Houghton, R.A., Scott, N.A., White, J.D., 2004. The net carbon flux due to deforestation and forest re-growth in the Brazilian Amazon: analysis using a process-based model. Global Change Biology 10, 908-924.

Houghton, R.A., 2005. Aboveground forest biomass and the global carbon balance. Global Change Biology 11, 945-958.

Houghton, R.A., Hackler, J.L., 1999. Emissions of carbon from forestry and land-use change in the tropical Asia. Global Change Biology 5, 481-492.

Houghton, R.A., Scole, D.L., Nobre, C.A., Hackler, J.L., Lawrence, K.T., Chomentowskl, W.H., 2000. Annual fluxes of carbon from deforestation and regrowth in the Brazilian Amazon. Nature 403, 301-304.

Huete, A.R. 1988. A soil-adjusted vegetation index (SAVI). Remote Sensing of Environment, 25, 89-105.

Inoue, Y., Olioso, A., 2006. Estimating dynamics of ecosystem CO2 flux and biomass production in agricultural field on the basis of synergy between process models and remotely sensed signatures. Journal of Geophysical Research 111, D24S91, doi:10.1029/2006JD007469.

Inoue, Y., Penuelas, J., Miyata, A., Mano, M., 2008a. Normalized difference spectral indices for estimating photosynthetic efficiency and capacity at a canopy scale derived from hyperspectral and CO_2 flux measurements in rice. Remote Sensing of Environment 112, 156-172.

Inoue, Y., Qi, J., Olioso, A., Kiyono, Y. Ochiai, Y., Saito, S., Asai, H., Horie, T., Shiraiwa, T., Dounagsavanh, L., 2008b. Reflectance characteristics of the major land surfaces in slash-and-burn ecosystems in Laos. International Journal of Remote Sensing 29, 2011-2019.

Inoue, Y., Qi, J., Olioso, A., Kiyono, Y., Ochiai, Y., Horie, T. Asai, H., Saito, K., Shiraiwa, T., Douangsavanh, L., 2007. Traceability of slash-and-burn land-use history using optical satellite sensor imagery: a basis for chrono-sequential assessment of ecosystem carbon stock in Laos. International Journal of Remote Sensing 28, 5641-5648.

IPCC National Greenhouse Gas Inventories Programme, 2003. Good Practice Guidance for Land Use, Land-Use Change and Forestry Institute for Global Environmental Strategies. Hayama, 1-275.

Jakobsen, J., Rasmussen, K., Leisz, S., Folving, R., Quang, N.V. 2007.The effects of land tenure policy on rural livelihoods and food sufficiency in the upland village of Que, North Central Vietnam. Agricultural Systems 94, 309-319.

Kiyono, Y., Ochiai, Y., Chiba, Y., Asai, H., Shiraiwa, T., Horie, T., Songnoukhai, V., Navongxai, V., Inoue, Y., 2007. Predicting chronosequential changes in carbon stocks of pachymorph bamboo communities in slash-and-burn agricultural fallow, northern Lao People's Democratic Republic. Journal of Forest Research 12, 371-383.

Lambin, E.F., 1999. Monitoring forest degradation in tropical regions by remote sensing: some methodological issues. Global Ecology and Biogeography 8, 191–198.

Meyfroidt, P., Lambin, E.F., 2008. Forest transition in Vietnam and its environmental impacts. Global Change Biology 14, 1-18.

Nagler, P.L., Inoue, Y., Glenn, E.P., Russ, A.L. and Daughtry, C.S.T., 2003. Cellulose absorption index (CAI) to quantify mixed soil–plant litter scenes, Remote Sensing of Environment, 87, 310-325.

Nakane, K., Yamamoto, M., Tsubota, H., 1983. Estimation of root respiration rate in a mature forest ecosystem. Japanese Journal of Ecology 33, 397-408.

Norgaard, L., Saudland, A., Wagner, J., Nielsen, J.P., Munck, L., Engelsen, S.B. 2000. Interval partial least-squares regression (iPLS): A comparative chemometric study with an example from near-infrared spectroscopy. Applied Spectroscopy, 54, 413-419.

Pearlman, J.S., Barry, P.S., Segal, C.C., Shepanski, J., Beiso, D., Carman, S.L. 2003. Hyperion, a space-based imaging spectrometer. IEEE Transactions on Geoscience and Remote Sensing, 41, 1160-1173.

Perez, C., Roncoli, C., Neely, C., Steiner, J.L. 2007. Can carbon sequestration markets benefit low-income producers in semi-arid Africa? Potentials and challenges. Agricultural Systems 94, 2-12.

Pravongvienkham, P., 2004. Upland natural resources management strategies and policy in the Lao PDR. In: Furukawa, H. (Ed.), Ecological destruction, Health, and Development: Advancing Asian Paradigms. Center for Southeast Asian Studies, Kyoto, pp. 481-501.

Qi, J., Chehbouni, A., Huete, A. R., Kerr, Y. H., Sorooshian, S. 1994. A modified soil adjusted vegetation index. Remote Sensing of Environment, 48, 119-126.

Ramankutty, N., Gibbs, H.K., Achard, F., Defries, R., Foley, J.A., Houghton, R.A., 2007. Challenges to estimating carbon emissions from tropical deforestation. Global Change Biology 13, 51-66.

Rasul, G., Gopal, G.B., 2003. Shifting cultivation in the mountains of south and Southeast Asia: Regional patterns and factors influencing the change. Land Degradation and Development 14, 495-508.

Righelato, R., Spracklen, D.V., 2007. Carbon mitigation by biofuels or by saving and restoring forests? Science 317, 902.

Roder, W., 2001. Slash-and-burn rice systems in the hills of northern Lao PDR: Description, challenges and opportunities. IRRI, Los Banos, pp.1-201.

Saito, K., Linquist, B., Atlin, G.N., Phanthaboon, K., Shiraiwa, T., Horie, T., 2006a. Response of traditional and improved upland rice cultivars to N and P fertilizer in northern Laos. Field Crops Research 96, 216-223.

Saito, K., Linquist, B., Keobualapha, B., Phanthaboon, K., Shiraiwa, T., Horie, T., 2006b. Stylosanthes guianensis as a short-term fallow crop for improving upland rice productivity in northern Laos. Field Crops Research 96, 438-447.

Shrestha, D.P., Zinck, J.A., 2001. Land use classification in mountainous areas: integration of image processing, digital elevation data and field knowledge (application to Nepal), International Journal of Applied Earth Observation and Geoinformation 3, 78-85.

Smith, J., van de Kop, P., Reategui, K., Lombardi, I., Sabogal, C., Diaz, A., 1999. Dynamics of secondary forests in slash-and-burn farming: interactions among land use types in the Peruvian Amazon. Agriculture, Ecosystems and Environment 76, 85–98.

Tian, H., Melillo, J.M., Kicklighter, D.W., Pan, S., Liu, J., McGuire, A.D., Moore, III. B., 2003. Regional carbon dynamics in monsoon Asia and its implications for the global carbon cycle. Global and Planetary Change 37, 201-217.

Tulaphitak, T., Pairintra, C., Kyuma, K., 1985. Changes in soil fertility and tilth under shifting cultivation. II. Changes in soil nutrient status. Soil Science and Plant Nutrition 31, 239-249.

Vargas, R., Allen, M.F., Allen, E.B., 2008. Biomass and carbon accumulation in a fire chronosequence of a seasonally dry tropical forest. Global Change Biology 14, 109-124.

Veroustraete, F., Sabbe, H., Eerens, H., 2002. Estimation of carbon mass fluxes over Europe using the C-Fix model and Euroflux data. Remote Sensing of Environment 83, 376-399.

Wicks, T.E., Smith, G.M., Curran, P.J., 2002. Polygon-based aggregation of remotely sensed data for regional ecological analyses, International Journal of Applied Earth Observation and Geoinformation 4, 161-173.